Chaos, Solitons and Fractals 176 (2023) 114101

Contents lists available at ScienceDirect

Chaos, Solitons and Fractals

journal homepage: www.elsevier.com/locate/chaos

Effects of the random walk and the maturation period in a diffusive predator–prey system with two discrete delays

Ş. Bilazeroğlu [a,*], S. Göktepe [b], H. Merdan [c]

[a] Çankaya University, Department of Mathematics, Ankara, Turkey
[b] Middle East Technical University, Department of Civil Engineering, Ankara, Turkey
[c] TOBB University of Economics and Technology, Department of Mathematics, Ankara, Turkey

ARTICLE INFO

Keywords:
Functional partial differential equations
Delay differential equations
Reaction–diffusion system
Discrete time delays
Hopf bifurcation
Stability
Periodic solutions
Population dynamics

ABSTRACT

This study aims to present a complete Hopf bifurcation analysis of a model describing the relationship between prey and predator. A ratio-dependent reaction–diffusion system with two discrete time delays operating under Neumann boundary conditions governs the model that represents this competition. The bifurcation parameter for the analysis is a delay parameter that reflects the amount of time needed for the predator to be able to hunt. Bilazeroğlu and Merdan's algorithm (Bilazeroğlu et al., 2021), which is developed by using the center manifold theorem and normal form theory, is used to establish the existence of Hopf bifurcations and also the stability of the bifurcating periodic solutions. The same procedure is used to illustrate some specific bifurcation properties, such as direction, stability, and period. Furthermore, by examining a model with constant coefficients, we also analyze how diffusion and the amount of time needed for prey to mature impact the model's dynamics. To support the obtained analytical results, we also run some numerical simulations. The results indicate that the dynamic of the mathematical model is significantly influenced by diffusion, the amount of time needed for the predator to gain the capacity to hunt, and the amount of time required for prey to reach maturity that the predator can hunt.

1. Introduction

Differential equations, which represent time continuously, are frequently used to describe the dynamics of predator–prey systems. For such a model, the following is a typical framework:

$$\frac{dY}{dt} = f(Y)Y - g(Y,Z)Z, \tag{1.1a}$$

$$\frac{dZ}{dt} = bg(Y,Z)Z - \mu Z. \tag{1.1b}$$

Here, Y and Z express the number of prey and the number of predators at time t, respectively. Also, b is trophic efficiency and μ is predator death rate [1]. Prey per capita growth rate which decreases with Y in most models is represented by the function f [2]. The trophic function g, also known as the "functional response" in the prey equation (Eq. (1.1a)) and the "numerical response" in the predator equation (Eq. (1.1b)), describes the relationship between the dynamics of the prey and predator in prey–predator models [1]. The function $g(Y,Z)$ in Eq. (1.1a) describes the quantity of prey biomass devoured by each predator per unit of time, whereas $bg(Y,Z)$ in Eq. (1.1b) reflects the per capita production rate of predators [3].

Akçakaya et al. [1] express that there are various ways to formulate the trophic function, including dependence on prey density alone (Lotka–Volterra type models), on the ratio of prey to predator densities (Abrams and Ginzburg [2]), and on prey and predator densities separately (see Table 1).

Akçakaya et al. [1] also discussed why ratio-dependent predator–prey models should be preferred. In this study, it is concluded that the majority of natural systems are closer to ratio dependence than prey dependency in light of the empirical evidence. Moreover, it is also stated in this study that a realistic simulation of prey–predator interactions ought to be able to forecast the full spectrum of dynamics seen in real-world prey–predator systems. The dynamics seen in the predator–prey relationship are contained in a ratio-dependent model because it

* Correspondence to: Çankaya University, Faculty of Science and Letters, Department of Mathematics, Eskişehir Yolu 29. Km. Yukarıyurtçu Mahallesi Mimar Sinan Caddesi No:4, 06790, Etimesgut, Ankara, Turkey.
E-mail addresses: sbilazeroglu@cankaya.edu.tr (Ş. Bilazeroğlu), sgoktepe@metu.edu.tr (S. Göktepe), merdan@etu.edu.tr (H. Merdan).

https://doi.org/10.1016/j.chaos.2023.114101
Received 10 August 2023; Received in revised form 20 September 2023; Accepted 22 September 2023
Available online 4 October 2023

Table 1
Some trophic function $g(Y,Z)$ examples [1].

Type	Equation	Source
Prey dependent	$g(Y,Z)=aY$	Lotka (1920) [6] - Volterra (1926) [7]
	$g(Y,Z)=aY/(b+Y)$	Holling (1959) [8]
	$g(Y,Z)=g(Y)$	Rosenzweig and MacArthur (1963) [9]
Intermediate	$g(Y,Z)=aYZ^{-m}$	Hassel and Varley (1969) [10]
	$g(Y,Z)=aY/(b+Y+cZ)$	DeAngelis et al. (1975) [11]
Ratio dependent	$g(Y,Z)=aY/(Y+cZ)$	Getz (1984) [12]
	$g(Y,Z)=g(Y/Z)$	Arditi and Ginzburg (1989) [13]

can feature stable equilibria, limit cycles, and the extinction of both species as a result of overexploitation [1]. As an example, Akçakaya [4] shows that a lynx-hare model lead to extinction for some parameter combinations. When the model is modified by adding a small prey refuge, dynamics changes extinction to limit cycles with period close to the observed period of lynx-hare cycles in Canada, with parameters estimated from field studies [4]. Akçakaya et al. [1] indicate that this type of prediction was never made by a Lotka–Volterra model for the lynx-hare system. Another reason emphasized by Akçakaya et al. [1] is that predators have to share preys. Modeling the functional response with a ratio (i.e., with "available resources per consumer") is a result of a direct sharing mechanism [1]. As a result, ratio-dependent models give a more realistic approach than prey-dependent models in many aspects.

2. Mathematical model

The Lotka–Volterra model, also known as the simplest predator–prey model, is

$$\begin{cases} \dfrac{dY(t)}{dt} = \alpha Y(t) - \beta Y(t)Z(t) \\ \dfrac{dZ(t)}{dt} = -\gamma Z(t) + \delta Y(t)Z(t), \end{cases} \tag{2.1}$$

where α, β, γ and δ are positive. The population densities of prey and predator at time t are represented by $Y(t)$ and $Z(t)$, respectively. According to this model, the number of prey changes based on their natural growth minus the rate at which they are hunted, while the number of predators changes based on growth caused by food availability minus natural mortality [5].

Leslie [14] changes the second equation in the model (2.1) as follows:

$$\begin{cases} \dfrac{dY(t)}{dt} = r_1 Y(t) - \varepsilon Y(t)Z(t) \\ \dfrac{dZ(t)}{dt} = Z(t)\left(r_2 - \theta \dfrac{Z(t)}{Y(t)}\right), \end{cases} \tag{2.2}$$

where r_1, r_2, ε and θ are positive parameters. The system (2.2) differs from the classical Lotka–Volterra model (2.1). According to Leslie [14], the results of the author's analysis (unpublished observations) of some data provided by Gause [15] for the growth in numbers of Paramecium caudatum and Paramecium aurelia cultures, in which the food supply consisted of a suspension of Bacillus pyocyaneus in a buffered medium, has offered the form of the second equation originally in the system (2.2).

The first equation in the system expresses the change in prey population density as the difference between the natural growth of the population at the rate of r_1 and the amount that is hunted at the rate of ε. The second equation states that the predator population has grown logistically. In this logistic growth, the carrying capacity is not constant and It relates to the density of the prey population proportionally. That is, the predator population gets smaller as the number of predators per prey increases and grows as it decreases. This situation distinguishes the model (2.2) from the Lotka–Volterra model (2.1). In addition, since the increase in the numbers of individuals in predator population depends on the number of predator per prey, this model is ratio-dependent.

Now we will address the studies on the model (2.2) in the literature. Zhou et al. [16] analyze the local stability of the unique positive equilibrium point $P^\star = (\frac{\theta r_1}{\varepsilon r_2}, \frac{r_1}{\varepsilon})$ of the system (2.2) and they look into how the Allee effects affect both the dynamics of the prey and the predator populations.

In nature, an individual belonging to the predator population may not be capable of hunting at birth. That is, the predator often needs a certain maturity to be able to hunt. Hence, to analyze the impact of past population members on the current predator population, Çelik [17] studied the following system

$$\begin{cases} \dfrac{dY(t)}{dt} = r_1 Y(t) - \varepsilon Y(t)Z(t) \\ \dfrac{dZ(t)}{dt} = Z(t)\left(r_2 - \theta \dfrac{Z(t-\tau)}{Y(t)}\right) \end{cases} \tag{2.3}$$

by adding the delay term to the predator variable in the predator–prey interaction term in the second equation of the system (2.2). In contrast, a predator can select its prey from population members who have attained a certain level of maturity. In other words, prey needs a certain amount of time to be hunted by predators. To include this fact in the model, Çelik [18] next considered the system below

$$\begin{cases} \dfrac{dY(t)}{dt} = r_1 Y(t) - \varepsilon Y(t)Z(t) \\ \dfrac{dZ(t)}{dt} = Z(t)\left(r_2 - \theta \dfrac{Z(t)}{Y(t-\tau)}\right) \end{cases} \tag{2.4}$$

by adding the lag term to the prey variable in the predator–predator interaction term in the second equation of the system (2.2).

Karaoğlu and Merdan [19] obtained the system

$$\begin{cases} \dfrac{dY(t)}{dt} = r_1 Y(t) - \varepsilon Y(t)Z(t) \\ \dfrac{dZ(t)}{dt} = Z(t)\left(r_2 - \theta \dfrac{Z(t-\tau_2)}{Y(t-\tau_1)}\right) \end{cases} \tag{2.5}$$

by including these two delay conditions into the one model. Karaoğlu and Merdan [20] took the delay term τ as the bifurcation parameter when $\tau_1 = \tau_2 = \tau$, and showed that the system (2.5) has periodic solutions by performing Hopf bifurcation analysis. In [19], it was investigated that Hopf bifurcation occurred in the system (2.5) when τ_2 varies, so the system (2.5) had periodic solutions. In addition, Karaoğlu and Merdan, in both studies, calculated the Poincaré normal form coefficient $c_1(0)$ of the system that enables to establish the characteristics of periodic solutions by using the calculation method for n-dimensional delayed differential equation systems given by Hassard et al. [21].

All these models ignore the spatial aspects of the predator–prey dynamics. According to Malchow et al. [22], there could be two reasons for this. First, the results of the non-spatial analysis apply to the case of spatially homogeneous, "well-mixed" populations. This usually represents situations where the relevant habitat is sufficiently small. Alternatively, the impact of spatial dimension(s) can be ignored in an unusual situation when the individuals of a given species remain fixed in space at any time and in any generation. Although these assumptions are acceptable to some populations, they are not always valid in the real world. According to Malchow et al. [22], populations of ecological species are not stable in space; their distribution is constantly changing as a result of environmental influences like wind in the case of airborne species, and/or individual motion.

A widely accepted and theoretically most developed approach for small-scale individual motion is the process called random walks. One of the main characteristics of this process is that the direction of the motion is chosen randomly at each step, and this feature has been a reason for discussion and criticism. Indeed, it is difficult to imagine a mammal or a bird or even an insect moving randomly. However, the random walk is just an abstract technique, meaning there is actually no necessity to associate each step in this theoretical procedure with the

real-life steps or movement of a living being. For example, consider the motion of a flying insect. Each of its short flights is highly motivated to search for food or avoid predators or look for mating partner or something else, and is not at all random. However, a range of factors unavoidably have an impact on any new flight or walk selection. Therefore, the direction of the next flight may only be slightly correlated with the direction of the previous flight. Moreover, under the assumption that external environmental conditions do not create any preference in the direction of movement, this loss of information accumulates with each new flight, and thus after a certain number of steps the correlation between flights will be completely lost. This heuristic estimation is compatible with some field observation data (see Root and Kareiva [23]). According to these data, a very close approach can be made to the motion of insects at an appropriate spatial scale with random walk. Obviously, this randomization of the motion is not restricted to insects and should be applicable to almost all other species. Moreover, Brockmann et al. [24] has shown that a very good approach to the movement of people can be obtained with random walks if it is considered on a relevant spatiotemporal scale (Malchow et al. [22]). Partial differential equation systems modeling population growth with random walk are generally referred to as reaction–diffusion systems (Allen [25]). Up until now, the study of diffusive predator–prey systems has been the focus of research in fields like ecology and mathematical biology (see, for example, [26–28], and references there in).

In the light of this information, to make the system (2.5) which discuss the predator–prey population dynamics more realistic, we consider the random walk procedure and obtain the following reaction–diffusion system

$$\begin{cases} \dfrac{\partial Y(x,t)}{\partial t} = d_1 \dfrac{\partial^2 Y(x,t)}{\partial x^2} + r_1 Y(x,t) - \varepsilon Y(x,t) Z(x,t) \\ \dfrac{\partial Z(x,t)}{\partial t} = d_2 \dfrac{\partial^2 Z(x,t)}{\partial x^2} + Z(x,t)\left(r_2 - \theta \dfrac{Z(x,t-\tau_2)}{Y(x,t-\tau_1)}\right) \end{cases} \tag{2.6}$$

with the following Neumann boundary conditions and initial conditions:

$$\begin{aligned} &\frac{\partial Y(x,t)}{\partial x} = \frac{\partial Z(x,t)}{\partial x} = 0, \quad x \in \{0,\pi\}, \quad t \geq 0, \\ &Y(x,t) = Y_0(x,t) \geq 0, \quad x \in [0,\pi], \quad t \in \left[-\tau_1, 0\right], \\ &Z(x,t) = Z_0(x,t) \geq 0, \quad x \in [0,\pi], \quad t \in \left[-\tau_2, 0\right], \end{aligned}$$

where $Y_0(x,t) \in C^2((0,\pi) \times \left[-\tau_1,0\right], \mathbb{R}) \cap C([0,\pi] \times \left[-\tau_1,0\right], \mathbb{R})$ and $Z_0(x,t) \in C^2((0,\pi) \times \left[-\tau_2,0\right], \mathbb{R}) \cap C([0,\pi] \times \left[-\tau_2,0\right], \mathbb{R})$. Here, $Y(x,t)$ and $Z(x,t)$ denote the adult population densities of prey and predator at position x and time t, respectively. $Y(x,t-\tau_1)$ and $Z(x,t-\tau_2)$ stand for the densities of juvenile prey and predator populations born at time $t-\tau_1$ and $t-\tau_2$, and surviving at time t and at position x, respectively. Positive parameters d_1 and d_2 are the diffusion coefficients of prey and predator, respectively. The positive parameters r_1, r_2, ε and θ symbolize the natural growth rate of the prey population, the hunting rate of the prey population, the natural growth rate of the predator population and the trophic efficiency, respectively. The positive real numbers τ_1 and τ_2, respectively, indicate the time required for prey to reach the maturity that the predator choose to hunt and the time required for the predator to have the ability to hunt. Neumann boundary conditions show that the prey and predator populations are in an isolated area, that is, there is no migration from outside to inside and inside to outside.

Hu and Li [29] performed the linear stability analysis of the system (2.6) when $\tau_1 = 0$ and the Hopf bifurcation existence analysis, and then they investigated the circumstances that would lead to the system having a periodic solution. In addition, they identified the characteristics of periodic solutions that are guaranteed to exist.

Our aim in this paper is to give a detailed Hopf bifurcation analysis of the system (2.6) for arbitrary τ_1 and τ_2. We investigate the linear stability, the existence and the direction of Hopf bifurcation using the algorithm develop in [30]. We use the Hopf bifurcation analysis and numerical simulations to study the effect of maturation periods and random walks of prey and predator on solutions of Eq. (2.6).

The paper has the following structure. In Section 3, it is discussed if a constant equilibrium point is stable and whether Hopf bifurcation exists. The bifurcation properties of the periodic solutions, including stability, direction, and period, are studied in Section 3.2. Finally, in Section 4, we consider a ratio-dependent reaction–diffusion system with constant coefficients including two discrete time delays under the Neumann boundary conditions. To support the analytical results, we executed some numerical simulations. Some concluding remarks are made at the end of the paper.

3. Hopf bifurcation analysis

In this section, stability of the unique positive equilibrium point $P^\star = (\frac{\theta r_1}{\varepsilon r_2}, \frac{r_1}{\varepsilon})$ of the system (2.6) and the conditions under which the system (2.6) has a periodic solution are investigated. Moreover, we determine the stability, direction, and also the period of the bifurcating periodic solutions.

System (2.6) belongs to a class of 2×2 reaction–diffusion equation systems containing two discrete delays which is fully analyzed in the sense of Hopf bifurcation by Bilazeroğlu and Merdan [30]. In this study, it is shown that one can determine the conditions for the existence of the Hopf bifurcation and compute the necessary values for the direction analysis of the Hopf bifurcation by calculating only coefficients in the second degree Taylor polynomials of the functions on the right-hand sides of the equations in the system (2.6). Because of that, we will apply the algorithm obtained by Bilazeroğlu and Merdan [30] to complete the analysis in this section.

3.1. Stability analysis and the existence of Hopf bifurcation

As we mentioned before, $P^\star = (\frac{\theta r_1}{\varepsilon r_2}, \frac{r_1}{\varepsilon})$ is the unique positive equilibrium point of the system (2.6). We examine stability of the equilibrium point $P^\star$ and the presence of Hopf bifurcation in the system (2.6) in three steps using the algorithm developed in [30] as follows: First, we get adequate conditions for all eigenvalues of characteristic equation having negative real parts when there is no delay. Second, when $\tau_2 = 0$, we obtain sufficient conditions to local asymptotic stability of equilibrium point $P^\star$ either for all $\tau_1 \geq 0$ or when $\tau_1 \in \left[0, \tau_{1_{j,0}}\right)$ for some $\tau_{1_{j,0}}$. In this step, since we deal with a single delay one can also use the algorithm improved by Kayan and Merdan in [31]. Finally, for fixed τ_1^* in its stability interval, we investigate the characteristic equation regarding τ_2 as a bifurcation value to find the stability region for equilibrium point $P^\star$ and bifurcation value $\tau_{2_0}(\tau_1^*) = \tau_{2_0}$ such that the real parts of all eigenvalues are still negative when $\tau_2 \in \left[0, \tau_{2,0}\right)$. After that, by analyzing transversality condition, we conclude the conditions under which a family of periodic solutions bifurcated from equilibrium point $P^\star$ at a critical value τ_{2_0}. In order to perform these steps, first of all we need to obtain characteristic equation.

Define the functions on the right-hand sides of the equations in the system (2.6) as

$$\begin{aligned} f(Y(x,t), Y(x,t-\tau_1), Z(x,t), Z(x,t-\tau_2)) &= r_1 Y(x,t) - \varepsilon Y(x,t) Z(x,t), \\ g(Y(x,t), Y(x,t-\tau_1), Z(x,t), Z(x,t-\tau_2)) &= Z(x,t)\left(r_2 - \theta \frac{Z(x,t-\tau_2)}{Y(x,t-\tau_1)}\right). \end{aligned} \tag{3.1}$$

Coefficients in the first degree Taylor polynomials at $P^\star$ of the function f can be calculated as

$$\begin{aligned} &k_1 = f_Y(P^\star) = 0, \qquad k_2 = f_{Y_{\tau_1}}(P^\star) = 0, \\ &k_3 = f_Z(P^\star) = -\frac{\theta r_1}{r_2}, \quad k_4 = f_{Z_{\tau_2}}(P^\star) = 0, \end{aligned} \tag{3.2a}$$

and of the function g can be calculated as

$$\begin{aligned} &l_1 = g_Y(P^\star) = 0, \quad l_2 = g_{Y_{\tau_1}}(P^\star) = \frac{r_2^2}{\theta}, \\ &l_3 = g_Z(P^\star) = 0, \quad l_4 = g_{Z_{\tau_2}}(P^\star) = -r_2, \end{aligned} \tag{3.2b}$$

where

$$f_{Y_{\tau_1}} = \frac{\partial f}{\partial Y(t-\tau_1)}, \quad f_{Z_{\tau_2}} = \frac{\partial f}{\partial Z(t-\tau_2)},$$
$$g_{Y_{\tau_1}} = \frac{\partial g}{\partial Y(t-\tau_1)}, \quad g_{Z_{\tau_2}} = \frac{\partial g}{\partial Z(t-\tau_2)}.$$

Formulas of the coefficients of the characteristic equation are given in [30] as

$$a = (d_1+d_2)\frac{n^2}{\ell^2} - (k_1+l_3), \quad b_1 = -d_2k_2\frac{n^2}{\ell^2} + k_2l_3 - k_3l_2,$$
$$b_2 = -d_1l_4\frac{n^2}{\ell^2} + k_1l_4 - k_4l_1, \quad c_1 = -k_2, \quad c_2 = -l_4,$$
$$d = d_1d_2\frac{n^4}{\ell^4} - (d_1l_3+d_2k_1)\frac{n^2}{\ell^2} + k_1l_3 - k_3l_1, \quad h = k_2l_4 - k_4l_2.$$

Consequently, the characteristic equation corresponding to the linearization of the system (2.6) around the equilibrium point *Pstar* is (see Section 3 in [30])

$$\lambda^2 + a\lambda + b_1e^{-\lambda\tau_1} + b_2e^{-\lambda\tau_2} + c_2\lambda e^{-\lambda\tau_2} + d = 0 \tag{3.3a}$$

where

$$a = (d_1+d_2)n^2, \quad b_1 = r_1r_2, \quad b_2 = d_1r_2n^2,$$
$$c_1 = 0, \quad c_2 = r_2, \quad d = d_1d_2n^4, \quad h = 0. \tag{3.3b}$$

To be able to obtain the first stability result, we check the hypothesis **(H1)** and **(H2)** of Corollary 1 given in Section 3.1 by Bilazeroğlu and Merdan [30]. Note that $a+c_1+c_2 = (d_1+d_1)n^2+r_2 > 0$ and $b_1+b_2+d+h = d_1d_2n^4 + d_1r_2n^2 + r_1r_2 > 0$, so hypothesis **(H1)** and **(H2)** are satisfied. Hence, all roots of the characteristic Eq. (3.3a) have negative real parts when $\tau_1 = \tau_2 = 0$ by Corollary 1 given in [30]. As a result, we have the undermentioned result:

Corollary 1. *The equilibrium point* $P^\star = (\frac{\theta r_1}{\varepsilon r_2}, \frac{r_1}{\varepsilon})$ *of the system (2.6) is locally asymptotically stable when* $\tau_1 = \tau_2 = 0$.

Now it is time to analyze the second case: $\tau_1 > 0$ and $\tau_2 = 0$. Using the following definitions given in [30] (see Equation (3.4) in [30])

$$R := \left(a+c_2\right)^2 - c_1^2 - 2\left(b_2+d\right) \quad \text{and} \quad S := \left(b_2+d\right)^2 - \left(b_1+h\right)^2,$$

and equalities in (3.3b), we calculate R and S as

$$R = (d_1^2+d_2^2)n^4 + 2d_2n^2r_2 + r_2^2, \tag{3.4a}$$
$$S = (d_1d_2n^4 + d_1n^2r_2 + r_1r_2)(d_1d_2n^4 + (d_1n^2 - r_1)r_2). \tag{3.4b}$$

Note that $R > 0$. Moreover, if $d_1n^2 - r_1 > 0$ then $S > 0$. Since $R > 0$ and $S > 0$ under the condition $d_1n^2 - r_1 > 0$, one of the following hypotheses of the Corollary 2 given in Section 3.1 by Bilazeroğlu and Merdan [30] is satisfied:

(H3-1) $R^2 - 4S < 0$,
(H3-2) $R^2 - 4S = 0$ and $R > 0$,
(H3-5) $R^2 - 4S > 0$, $R > 0$ and $S > 0$.

Moreover, if $d_1d_2n^4 + d_1n^2r_2 = r_1r_2$ then $S = 0$. So, under this condition the hypothesis "**(H3-4)** $R > 0$ and $S = 0$" of the Corollary 2 given in [30] holds. Therefore, we can conclude that:

Corollary 2. *If*

(H̃3-1) $d_1n^2 - r_1 > 0$,
(H̃3-2) $d_1d_2n^4 + d_1n^2r_2 = r_1r_2$

holds, then all roots of the characteristic Eq. (3.3a) have negative real parts for all $\tau_1 \geq 0$ *when* $\tau_2 = 0$. *It follows that the equilibrium point* $P^\star$ *is absolutely stable when* $\tau_2 = 0$. *Therefore, if one of the conditions* ***(H̃3-1)*** *or* ***(H̃3-2)*** *is satisfied, then the Hopf bifurcation will not occur in the system (2.6) when* $\tau_2 = 0$.

On the other hand, when $d_1 = d_2 = 0$, from Eq. (3.4b) we get that $S = -r_1^2r_2^2 < 0$. So, for sufficiently small values of d_1 and d_2, we have negative values for S. This means that for sufficiently small values of d_1 and d_2, only the hypothesis **(H4-2)** of Corollary 3 given in Section 3.1 by Bilazeroğlu and Merdan [30] (see Section 3.1 in [30]) is satisfied. For this reason, we have the conclusion next in line:

Corollary 3. *Assume that the undermentioned hypothesis is satisfied:*
(H̃4)] $S = (d_1d_2n^4 + d_1n^2r_2 + r_1r_2)(d_1d_2n^4 + (d_1n^2 - r_1)r_2) < 0$. *This hypothesis automatically holds if* d_1 *and* d_2 *are sufficiently small positive real numbers. In this case, the followings hold.*

1. *Characteristic Eq. (3.3a) has a pair of purely imaginary roots* $\lambda_2(\tau_{1_{2,k}}) = i\omega_2$ *and* $\bar{\lambda}_2(\tau_{1_{2,k}}) = -i\omega_2$, $\omega_2 > 0$ *when* $\tau_2 = 0$ *where*

$$\omega_2 = \sqrt{\frac{-R \pm \sqrt{R^2 - 4S}}{2}}, \tag{3.5}$$

in which R *and* S *are specified by (3.4a) and (3.4b), respectively, and for* $k \in \mathbb{N}_0$

$$\tau_{1_{2,k}} = \frac{1}{\omega_2}\arctan\left(\frac{((d_1+d_2)n^2 + r_2)\omega_2}{\omega_2^2 - d_1d_2n^4 - d_1n^2r_2}\right) + \frac{k\pi}{\omega_2}. \tag{3.6a}$$

One can also calculate the bifurcation value using formulas given below:

$$\tau_{1_{2,k}} = \frac{1}{\omega_2}\arcsin\left(\frac{((d_1+d_2)n^2 + r_2)\omega_2}{r_1r_2}\right) + \frac{2k\pi}{\omega_2}, \tag{3.6b}$$
$$\tau_{1_{2,k}} = \frac{1}{\omega_2}\arccos\left(\frac{\omega_2^2 - d_1d_2n^4 - d_1n^2r_2}{r_1r_2}\right) + \frac{2k\pi}{\omega_2}. \tag{3.6c}$$

Also, the first delay value at which a pair of purely imaginary roots occurs is $\tau_{1_{2,0}}$.

2. $P^\star$ *is locally asymptotically stable for* $\tau_1 \in \left[0, \tau_{1_{2,0}}\right)$ *when* $\tau_2 = 0$ *and unstable for* $\tau_1 > \tau_{1_{2,0}}$ *when* $\tau_2 = 0$.
3. *Except the pair of purely imaginary roots* $\lambda_2(\tau_{1_{2,k}}) = i\omega_2$ *and* $\bar{\lambda}_2(\tau_{1_{2,k}}) = -i\omega_2$, *all roots of the characteristic Eq. (3.3a) have negative real parts at* $\tau_1 = \tau_{1_{2,0}}$ *when* $\tau_2 = 0$.
4. $\mathrm{Re}\left(\frac{d\lambda}{d\tau_1}\Big|_{\tau_1=\tau_{1_{2,0}}}\right) > 0$ *when* $\tau_2 = 0$.
5. *Hopf bifurcation occurs in system (2.6) at* $\tau_1 = \tau_{1_{2,0}}$ *when* $\tau_2 = 0$, *which means that the system (2.6) has a family of periodic solutions in a neighborhood of* $\tau_{1_{2,0}}$ *when* $\tau_2 = 0$.

Now, the stability interval of the equilibrium point $P^\star$ when $\tau_2 = 0$ has been determined. We can fix τ_1 as $\tau_1^* \in [0, \infty)$ if one of the conditions **(H̃3-i)**, $i = 1, 2$ holds or as $\tau_1^* \in \left[0, \tau_{1_{2,0}}\right)$ if d_1 and d_2 are sufficiently small. Note that the coefficients of the characteristic Eq. (3.3a) will certainly provide one of these conditions.

It is time to investigate the effect of τ_2 on the dynamics of the system (2.6), after fixing τ_1 in its stability interval. We have concluded that equilibrium point $P^\star$ is asymptotically stable for the fixed τ_1^* when $\tau_2 = 0$. So, $P^\star$ becomes unstable as τ_2 increases from 0 to ∞, if the characteristic Eq. (3.3a) has either a simple zero root or a pair of simple purely imaginary roots. Nonetheless, having (3.3a) a zero root contradicts to the fact that $b_1 + b_2 + d + h = d_1d_2n^4 + d_1r_2n^2 + r_1r_2 > 0$.

On the other side, $b_1 - b_2 + d - h = d_1d_2n^4 - d_n^2r_2 + r_1r_2 < 0$ then the hypothesis "**(H5)** $(b_1 - b_2 + d - h) < 0$" of Theorem 4 given in Section 3.1 by Bilazeroğlu and Merdan [30] holds. Therefore, there exist a sequence $\tau_{2_i} = \{\tau_{2_i}(\tau_1^*) | i = 1, 2, \ldots, r\}$ at which (3.3a) holds for every fixed $(\tau_{2_i}, \pm i\omega_i)$, $i = 1, 2, \ldots, r$. Let

$$\tau_{2_0} = \tau_{2_0}\left(\tau_1^*\right) = \min\left\{\tau_{2_i}\left(\tau_1^*\right) | i = 1, 2, \ldots, r\right\} \tag{3.7}$$

and $i\omega_0 = i\omega_0\left(\tau_{2_0}\right)$ is the associated purely imaginary eigenvalue. Consequentially, if the condition **(H̃5)** $d_1d_2n^4 - d_n^2r_2 + r_1r_2 < 0$ holds then

the characteristic Eq. (3.3a) has a pair of purely imaginary eigenvalue which is defined in a neighborhood of τ_{2_0} as

$$\lambda_0(\tau_2) = \alpha_0(\tau_2) + i\omega_0(\tau_2) \quad \text{and} \quad \overline{\lambda_0}(\tau_2) = \alpha_0(\tau_2) - i\omega_0(\tau_2),$$

where

$$\alpha_0(\tau_{2_0}) = 0 \quad \text{and} \quad \omega_0(\tau_{2_0}) = \omega_0 > 0$$

for each τ_1 in its stability interval, i.e., $\tau_1 \in [0, \infty)$ if one of the conditions **(H̃3-i)**, $i = 1, 2$ holds or $\tau_1 \in \left[0, \tau_{1_{2,0}}\right)$ if d_1 and d_2 are sufficiently small. Note that all other roots of the characteristic Eq. (3.3a) have nonzero real parts at $\tau_2 = \tau_{2_0}$ because we uniquely determine τ_{2_0} such that $\lambda(\tau_{2_0}) = i\omega_0$, $\omega_0 = \omega_0(\tau_{2_0}) > 0$.

It is time to guarantee that $\pm i\omega_0$ is a simple root of characteristic Eq. (3.3a), in other words equilibrium point becomes unstable after the bifurcation value. If the hypothesis **(H6)** $\mathrm{Re}(P)\,\mathrm{Re}(Q) + \mathrm{Im}(P)\,\mathrm{Im}(Q) \neq 0$ of Theorem 4 given in Section 3.1 by Bilazeroğlu and Merdan [30] holds then we can conclude that $\mathrm{Re}\left(\left.\frac{d\lambda}{d\tau_2}\right|_{\tau_2=\tau_{2_0}}\right) \neq 0$. Using the formula (B.7) in Appendix B given in [30], we obtain the following formula:

$$\begin{aligned}
&\mathrm{Re}(P)\,\mathrm{Re}(Q) + \mathrm{Im}(P)\,\mathrm{Im}(Q)\\
&\quad = -r_1^2 r_2^4 \omega_0 + r_2^2\left(d_1^2 n^4 + \omega_0^2\right)^2 \omega_0\\
&\quad - r_1 r_2^3 n^2\left(d_1 + d_2\right)\left[\tau_1^* \omega_0^3 + d_1 n^2\left(2 + d_1 n^2 \tau_1^*\right)\omega_0\right]\cos(\tau_1^*\omega_0)\\
&\quad + r_1 r_2^3 \tau_1^* \omega_0^4 \sin(\tau_1^*\omega_0)\\
&\quad - r_1 r_2^3 n^2\left[\left(d_2 - d_1\right) d_1 n^2 \tau_1^* - \left(d_1 + d_2\right)\right]\omega_0^2 \sin(\tau_1^*\omega_0)\\
&\quad - d_1^2 r_1 r_2^3 n^6\left(d_1 d_2 n^2 \tau_1^* + d_1 + d_2\right)\sin(\tau_1^*\omega_0).
\end{aligned} \tag{3.8}$$

In conclusion, using formulas and calculations given in [30] we have the result given below:

Corollary 4. *Assume that*

(H̃5) $d_1 d_2 n^4 - d_n^2 r_2 + r_1 r_2 < 0$ *is satisfied. In that case, for each* τ_1 *in its stability interval, i.e.,* $\tau_1 \in [0, \infty)$ *if one of the conditions* ***(H̃3-i)****,* $i = 1, 2$ *holds or* $\tau_1 \in \left[0, \tau_{1_{2,0}}\right)$ *if* ***(H̃4)*** d_1 *and* d_2 *are sufficiently small, the followings hold:*

1. *Characteristic Eq. (3.3a) has a unique pair of purely imaginary roots* $\lambda(\tau_{2_0}(\tau_1)) = i\omega_0$ *and* $\overline{\lambda}(\tau_{2_0}(\tau_1)) = -i\omega_0$, $\omega_0 > 0$ *at some* $\tau_{2_0} > 0$. *Here,* ω_0 *is the root of*

$$\begin{aligned}
&\omega^4 + \left(a^2 - c_2^2 - 2d\right)\omega^2 + \left(b_1^2 - b_2^2 + d^2\right)\\
&\quad + 2b_1(-\omega^2 + d)\cos(\tau_1\omega) - 2ab_1\omega\sin(\tau_1\omega) = 0
\end{aligned} \tag{3.9}$$

and

$$\tau_{2_0}(\tau_1) = \frac{1}{\omega_0}\arctan\left(\frac{\phi_1(\tau_1)}{\phi_2(\tau_1)}\right), \tag{3.10a}$$

where

$$\begin{aligned}
\phi_1(\tau_1) &= c_2\omega_0^3 + (ab_2 - c_2 d)\omega_0 - b_1 c_2\omega_0\cos(\omega_0\tau_1) - b_1 b_2\sin(\omega_0\tau_1),\\
\phi_2(\tau_1) &= \left(-ac_2 + b_2\right)\omega_0^2 - b_2 d - b_1 b_2\cos(\omega_0\tau_1) + b_1 c_2\omega_0\sin(\omega_0\tau_1).
\end{aligned}$$

In addition, this value can be calculated with the undermentioned equations:

$$\tau_{2_0}(\tau_1) = \frac{1}{\omega_0}\arcsin\left(\frac{\phi_1(\tau_1)}{c_2^2\omega_0^2 + b_2^2}\right), \tag{3.10b}$$

$$\tau_{2_0}(\tau_1) = \frac{1}{\omega_0}\arccos\left(\frac{\phi_2(\tau_1)}{c_2^2\omega_0^2 + b_2^2}\right). \tag{3.10c}$$

2. *Except the pair of purely imaginary roots* $\lambda(\tau_{2_0}(\tau_1)) = i\omega_0$ *and* $\overline{\lambda}(\tau_{2_0}(\tau_1)) = -i\omega_0$, *all roots of the characteristic Eq. (3.3a) have negative real parts at* $\tau_2 = \tau_{2_0}(\tau_1)$.
3. *If* ***(H̃6)*** $\mathrm{Re}(P)\,\mathrm{Re}(Q) + \mathrm{Im}(P)\,\mathrm{Im}(Q) \neq 0$ *is satisfied then we have*

$$\mathrm{Re}\left(\left.\frac{d\lambda_0}{d\tau_2}\right|_{\tau_2=\tau_{2_0}}\right) = \alpha_0'(\tau_{2_0}) \neq 0.$$

Hence, the transversality condition holds. Here, formula of

$$\mathrm{Re}(P)\,\mathrm{Re}(Q) + \mathrm{Im}(P)\,\mathrm{Im}(Q)$$

is given by Eq. (3.8).

Thus, using Theorem 4 given by [30] (see Section 3.1 in [30]), we can reach the conclusion given below about the existence of periodic solutions of the system (2.6).

Theorem 5 (*Existence*). *Assume that the condition* ***(H̃5)*** $d_1 d_2 n^4 - d_n^2 r_2 + r_1 r_2 < 0$ *holds. Define the conditions which depend on the coefficients of the characteristic Eq. (3.3a) as* ***(H̃3-1)*** $d_1 n^2 - r_1 > 0$ ***(H̃3-2)*** $d_1 d_2 n^4 + d_1 n^2 r_2 = r_1 r_2$, ***(H̃4)*** *"*$d_1$ *and* d_2 *are sufficiently small positive real numbers".*

Then, the following results hold for each $\tau_1 \in [0, \infty)$ *if one of the conditions* ***(H̃3-i)****,* $i = 1, 2$ *is satisfied or for each* $\tau_1 \in \left[0, \tau_{1_{2,0}}\right)$ *if* ***(H̃4)*** *is satisfied.*

1. *Equilibrium point* $P^\star = (\frac{\theta r_1}{\varepsilon r_2}, \frac{r_1}{\varepsilon})$ *is locally asymptotically stable when* $\tau_2 \in [0, \tau_{2_0})$ *where* $\tau_{1_{2,0}}$ *and* $\tau_{2_0} = \tau_{2_0}(\tau_1)$ *are given by (3.6a) and (3.10a), respectively. In other words,* $P^\star$ *is locally asymptotically stable at the points* (τ_1, τ_2) *belonging to the region below the graph of* $\tau_{2_0} = \tau_{2_0}(\tau_1)$. $P^\star$ *is unstable when* $\tau_2 > \tau_{2_0}(\tau_1)$.
2. *If the condition* ***(H̃6)*** $\mathrm{Re}\,P\,\mathrm{Re}\,Q + \mathrm{Im}\,P\,\mathrm{Im}\,Q \neq 0$ *is also satisfied where the formula of* $(\mathrm{Re}(P)\,\mathrm{Re}(Q) + \mathrm{Im}(P)\,\mathrm{Im}(Q))$ *is given in by (3.8), then the equilibrium point* $P^\star$ *is unstable when* $\tau_2 > \tau_{2_0}$. *In addition to that, the (2.6) undergoes a Hopf bifurcation at the equilibrium point* $P^\star$ *which means that a family of periodic solutions appears out of the equilibrium point* $P^\star$ *as the delay parameter* τ_2 *passes through* τ_{2_0}.

3.2. Direction and stability of Hopf bifurcation

In the previous section, we discovered the circumstances in which the delayed predator–prey model experiences the Hopf bifurcation. We will examine the direction of Hopf bifurcation as well as the stability of the bifurcating periodic solutions in this section. Since the system is in the class of reaction diffusion system with two discrete delays which is studied by Bilazeroğlu and Merdan [30], instead of reducing the system (2.6) to the central manifold, we will use the algorithm demonstrated by Bilazeroğlu and Merdan [30] (see Section 3.2 in [30]) to determine the characteristics of periodic solutions.

Throughout this section, we assume that Hopf bifurcation arises in the system (2.6) when τ_2 passes through the bifurcation value τ_{2_0} given by (3.10a), i.e., it satisfies the hypotheses of Theorem 5. Also, we shift the bifurcation value to the zero via the transformation $\tau_2 = \tau_{2_0} + \mu$.

Since the characteristic Eq. (3.2a) of the system (2.6) is an exponential polynomial, the system (2.6) has infinite dimension. To be able to analyze such a system, firstly we reduce it to single ordinary differential equation in one complex variable on a center manifold at the bifurcation value $\mu = 0$. To do this, define the new variable as

$$\mathbf{U}_t = z(t)q + \overline{z}(t)\overline{q} + w.$$

Here, $\mathbf{U}_t(\theta) = \mathbf{U}(t+\theta)$ where $\mathbf{U}(t) = (Y(t) - \frac{\theta r_1}{\varepsilon r_2}, Z(t) - \frac{r_1}{\varepsilon})^T$, $z(t) = \langle q^*, \mathbf{U}_t\rangle \in \mathbb{C}$ and $\langle q^*, w\rangle = 0$. In the variables z and w, at the bifurcation value $\mu = 0$ the system (2.6) turns to

$$\begin{cases} \dot{z} = i\omega_0 z + g(z, \overline{z}; 0), \\ \dot{w} = A(0)w + H(z, \overline{z}; 0), \end{cases}$$

where

$$g(z, \overline{z}; 0) = \sum_{i+j=2}^{k} g_{ij}(0)\frac{z^i \overline{z}^j}{i!\,j!} + \mathcal{O}(|z|^{k+1}) = \overline{q^*}(0)\cdot h(z, \overline{z}; 0), \tag{3.11}$$

and

$$H(z, \overline{z}, 0) = \begin{cases} -g(z, \overline{z}; 0)q(\theta) - \overline{g}(z, \overline{z}; 0)\overline{q}(\theta), & \theta \in [-\tau_m, 0) \\ h(z, \overline{z}; 0) - g(z, \overline{z}; 0)q(0) - \overline{g}(z, \overline{z}; 0)\overline{q}(0), & \theta = 0. \end{cases}$$

Here, $q(\theta)$ is an eigenvector of $A(0)$ corresponding to $\lambda(0) = i\omega_0$ and $q^*(\sigma)$ is an eigenvector of $A^*(0)$ corresponding to $\overline{\lambda(0)} = -i\omega_0$, where

$\lambda(\mu) = \alpha(\mu) + i\omega(\mu)$ is the simple complex eigenvalue of the system (2.6) with $\alpha(0) = 0$ and $\omega(0) = \omega_0$. $A(0)$ is the operator defined for $\phi \in D^1 = C^1\left([-\tau_m, 0], \mathbb{R}^2\right)$ as

$$A(\mu)\phi(\theta) = \begin{cases} \dfrac{d\phi(\theta)}{d\theta}, & \theta \in [-\tau_m, 0), \\ \int_{-\tau_m}^{0} d\eta(\mu, \nu)\phi(\nu), & \theta = 0, \end{cases}$$

Here,

$$d\eta(\mu, \theta) = \left(B\delta(\theta) + C\delta(\theta + \tau_1^*) + D\delta(\theta + \mu + \tau_{2_0})\right) d\theta,$$

where $\delta(\theta)$ is the Dirac delta function and

$$B = \begin{pmatrix} -d_1\frac{n^2}{\ell^2} + k_1 & k_3 \\ l_1 & -d_2\frac{n^2}{\ell^2} + l_3 \end{pmatrix}, \quad C = \begin{pmatrix} k_2 & 0 \\ l_2 & 0 \end{pmatrix},$$
$$D = \begin{pmatrix} 0 & k_4 \\ 0 & l_4 \end{pmatrix},$$

$A^*(\mu)$ is adjoint operator of $A(\mu)$ and is defined for $\psi = (\psi_1, \psi_2)^T \in \mathcal{E}^1$ in which $\mathcal{E} = C\left([0, \tau_m], \mathbb{R}^2\right)$ as

$$A^*(\mu)\psi(\sigma) = \begin{cases} -\dfrac{d\psi(\sigma)}{d\sigma}, & \sigma \in (0, \tau_m], \\ \int_{-\tau_m}^{0} d\eta^T(\mu, \nu)\psi(-\nu), & \sigma = 0. \end{cases}$$

Moreover, the function $h(z, \bar{z}; 0)$ is given by the equation (C.23) in Appendix C.3 in [30]. For the details of this reduction and calculations, one can see Appendix C in [30].

In order to determine the properties of periodic solutions, we need to calculate the coefficient $c_1(0)$ of the Poincaré normal form which is

$$c_1(0) = \frac{i}{2\omega_0}\left(g_{20}(0)g_{11}(0) - 2|g_{11}(0)|^2 - \frac{1}{3}|g_{02}(0)|^2\right) + \frac{1}{2}g_{21}(0).$$

We shall use the algorithm obtained in [30] to obtain the explicit formulas for the terms $g_{20}(0)$, $g_{11}(0)$, $g_{02}(0)$ and $g_{21}(0)$ (the coefficients in the expansion (3.11)).

First of all, we stand to calculate the coefficients in the second degree Taylor polynomials at $P^\star$ of the functions f and g (see Eqs. (3.1)). Coefficients in the first degree Taylor polynomials at $P^\star$ of the functions f and g are given by (3.2a) and (3.2b), respectively. And the coefficients of the quadratic terms in the second degree Taylor polynomials at $P^\star$ of the function f are obtained as (see Formulas (C.6) in Appendix C in [30])

$$\begin{aligned} &m_{11} = m_{12} = m_{14} = m_{22} = m_{23} = m_{33} = m_{34} = m_{44} = 0, \\ &m_{13} = -\varepsilon, \end{aligned} \tag{3.12a}$$

and of the function g are obtained as

$$\begin{aligned} &r_{11} = r_{12} = r_{13} = r_{14} = r_{33} = r_{44} = 0, \\ &r_{22} = -\frac{\varepsilon r_2^3}{\theta^2 r_1}, \quad r_{23} = r_{24} = \frac{\varepsilon r_2^2}{\theta r_1}, \quad r_{34} = -\frac{\varepsilon r_2}{r_1}. \end{aligned} \tag{3.12b}$$

The undermentioned formulas are valid for each $\tau_1 \in [0, \infty)$ if one of the conditions **(H̃3-i)**, $i = 1, 2$ holds or for each $\tau_1 \in \left[0, \tau_{1_{2,0}}\right)$ if **(H̃4)** holds.

As defined in [30] (see Appendix C), $q(\theta)$ and $q^*(\sigma)$ are

$$q(\theta) = \begin{pmatrix} 1 \\ c \end{pmatrix} e^{i\omega_0\theta} \quad \text{and} \quad q^*(\sigma) = s\begin{pmatrix} c^* \\ 1 \end{pmatrix} e^{i\omega_0\sigma}$$

where c, c^* and s are calculated using the formulas (C.15), (C.16) and (C.18), respectively, given in Appendix C by [30] as:

$$\begin{aligned} c &= -\frac{(i\omega_0 + d_1n^2)r_2}{\theta r_1}, \\ c^* &= \frac{(i\omega_0 - d_2n^2 - r_2e^{i\omega_0\tau_{2_0}})r_2}{\theta r_1}, \\ \bar{s} &= \left(c + \overline{c^*} + \tau_1 e^{-i\omega_0\tau_1}\frac{r_2^2}{\theta} - \tau_{2_0}e^{-i\omega_0\tau_{2_0}}r_2c\right)^{-1}. \end{aligned} \tag{3.13a}$$

To calculate the terms $g_{20}(0)$, $g_{11}(0)$ and $g_{02}(0)$ in the formula of the Poincaré normal form coefficient $c_1(0)$, we need to get the terms $h_{20}(0)$, $h_{11}(0)$ and $h_{02}(0)$. With the formulas (C.24a)-(C.24f) given in Appendix C by [30], we obtain these terms as:

$$\begin{aligned} h_{20_1}(0) &= -\varepsilon c \\ h_{20_2}(0) &= -\frac{\varepsilon r_2^3}{\theta^2 r_1}e^{-2i\omega_0\tau_1} + \frac{\varepsilon r_2^2}{\theta r_1}c\left(e^{-i\omega_0\tau_1} + e^{-i\omega_0(\tau_1+\tau_{2_0})}\right) - \frac{\varepsilon r_2}{r_1}c^2e^{-i\omega_0\tau_{2_0}} \\ h_{11_1}(0) &= -\varepsilon\left(c + \bar{c}\right) \\ h_{11_2}(0) &= -\frac{2\varepsilon r_2^3}{\theta^2 r_1} + \frac{\varepsilon r_2^2}{\theta r_1}\left(c\left(e^{i\omega_0\tau_1} + e^{i\omega_0(\tau_1-\tau_{2_0})}\right) + \bar{c}\left(e^{-i\omega_0\tau_1} + e^{-i\omega_0(\tau_1-\tau_{2_0})}\right)\right) \\ &\quad - \frac{\varepsilon r_2}{r_1}c\bar{c}\left(e^{-i\omega_0\tau_{2_0}} + e^{i\omega_0\tau_{2_0}}\right) \\ h_{02_1}(0) &= -\varepsilon\bar{c} \\ h_{02_2}(0) &= -\frac{\varepsilon r_2^3}{\theta^2 r_1}e^{2i\omega_0\tau_1} + \frac{\varepsilon r_2^2}{\theta r_1}\bar{c}\left(e^{i\omega_0\tau_1} + e^{i\omega_0(\tau_1+\tau_{2_0})}\right) - \frac{\varepsilon r_2}{r_1}\bar{c}^2e^{i\omega_0\tau_{2_0}} \end{aligned} \tag{3.13b}$$

where c is given by (3.13a). Therefore, using the formulas (3.21a)-(3.21c) given in [30], we achieve the desired terms as:

$$\begin{aligned} g_{20}(0) &= 2\bar{s}\left[h_{20_1}(0)\overline{c^*} + h_{20_2}(0)\right], \\ g_{11}(0) &= \bar{s}\left[h_{11_1}(0)\overline{c^*} + h_{11_2}(0)\right] \\ g_{02}(0) &= 2\bar{s}\left[h_{02_1}(0)\overline{c^*} + h_{02_2}(0)\right]. \end{aligned} \tag{3.13c}$$

We have one more unknown term in the formula of the Poincaré normal form coefficient $c_1(0)$, namely,

$$g_{21}(0) = 2\bar{s}\left[h_{21_1}(0)\overline{c^*} + h_{21_2}(0)\right]. \tag{3.13d}$$

This formula is given by the Equation (3.21d) in [30]. In order to obtain $h_{21_1}(0)$ and $h_{21_2}(0)$, first of all, using the formula (3.22) given in [30] we calculate

$$\begin{aligned} W_{20}(0;0) &= -\frac{1}{i\omega_0}g_{20}(0)\begin{pmatrix} 1 \\ c \end{pmatrix} - \frac{1}{3i\omega_0}\overline{g}_{02}(0)\begin{pmatrix} 1 \\ \bar{c} \end{pmatrix} + K_{20}, \\ W_{20}(-\tau_1;0) &= -\frac{1}{i\omega_0}g_{20}(0)\begin{pmatrix} 1 \\ c \end{pmatrix}e^{-i\omega_0\tau_1} - \frac{1}{3i\omega_0}\overline{g}_{02}(0)\begin{pmatrix} 1 \\ \bar{c} \end{pmatrix}e^{i\omega_0\tau_1} \\ &\quad + K_{20}e^{-2i\omega_0\tau_1} \\ W_{20}(-\tau_{2_0};0) &= -\frac{1}{i\omega_0}g_{20}(0)\begin{pmatrix} 1 \\ c \end{pmatrix}e^{-i\omega_0\tau_{2_0}} - \frac{1}{3i\omega_0}\overline{g}_{02}(0)\begin{pmatrix} 1 \\ \bar{c} \end{pmatrix}e^{i\omega_0\tau_{2_0}} \\ &\quad + K_{20}e^{-2i\omega_0\tau_{2_0}} \end{aligned} \tag{3.13e}$$

where

$$\begin{aligned} D_{20} &= -4\omega_0^2 + 2i\omega_0\left((d_1 + d_2)n^2 + r_2e^{-2i\omega_0\tau_{2_0}}\right) + d_1d_2n^4 \\ &\quad + r_1r_2e^{-2i\omega_0\tau_1} + d_1r_2n^2e^{-2i\omega_0\tau_{2_0}} \\ K_{20} &= \frac{2}{D_{20}}\begin{pmatrix} \left(2i\omega_0 + d_2n^2 + r_2e^{-2i\omega_0\tau_{2_0}}\right)h_{20_1}(0) - \dfrac{\theta r_1}{r_2}h_{20_2}(0) \\ \dfrac{r_2^2}{\theta}h_{20_1}(0)e^{-2i\omega_0\tau_1} + \left(2i\omega_0 + d_1n^2\right)h_{20_2}(0) \end{pmatrix} \end{aligned}$$

and using the formula (3.23) given in [30] we get

$$\begin{aligned} W_{11}(0;0) &= \frac{1}{i\omega_0}g_{11}(0)\begin{pmatrix} 1 \\ c \end{pmatrix} - \frac{1}{i\omega_0}\overline{g}_{11}(0)\begin{pmatrix} 1 \\ \bar{c} \end{pmatrix} + K_{11}, \\ W_{11}(-\tau_1;0) &= \frac{1}{i\omega_0}g_{11}(0)\begin{pmatrix} 1 \\ c \end{pmatrix}e^{-i\omega_0\tau_1} - \frac{1}{i\omega_0}\overline{g}_{11}(0)\begin{pmatrix} 1 \\ \bar{c} \end{pmatrix}e^{i\omega_0\tau_1} + K_{11} \\ W_{11}(-\tau_{2_0};0) &= \frac{1}{i\omega_0}g_{11}(0)\begin{pmatrix} 1 \\ c \end{pmatrix}e^{-i\omega_0\tau_{2_0}} - \frac{1}{i\omega_0}\overline{g}_{11}(0)\begin{pmatrix} 1 \\ \bar{c} \end{pmatrix}e^{i\omega_0\tau_{2_0}} + K_{11} \end{aligned} \tag{3.13f}$$

where

$$K_{11}=\frac{1}{(d_1d_2n^4+d_1r_2n^2+r_1r_2)}\begin{pmatrix}\left(d_2n^2+r_2\right)h_{11_1}(0)-\dfrac{\theta r_1}{r_2}h_{11_2}(0)\\ \dfrac{r_2^2}{\theta}h_{11_1}(0)+d_1n^2h_{11_2}(0)\end{pmatrix}.$$

Eventually, formulas (C.24 g) and (C.24 h) given in Appendix C by [30] yield the following projected equations:

$$\begin{aligned}h_{21_1}(0)=&-\varepsilon\left[\frac{1}{2}W_{20_1}(0)\bar{c}+W_{11_1}(0)c+\frac{1}{2}W_{20_2}(0)+W_{11_2}(0)\right]\\ h_{21_2}(0)=&-\frac{\varepsilon r_2^3}{\theta^2r_1}\left[W_{20_1}\left(-\tau_1\right)e^{i\omega_0\tau_1}+2W_{11_1}\left(-\tau_1\right)e^{-i\omega_0\tau_1}\right]\\ &+\frac{\varepsilon r_2^2}{\theta r_1}\left[\frac{1}{2}W_{20_1}(-\tau_1)\bar{c}+W_{11_1}\left(-\tau_1\right)c+\frac{1}{2}W_{20_2}(0)e^{i\omega_0\tau_1}\right.\\ &\left.+\ W_{11_2}(0)e^{-i\omega_0\tau_1}\right]\\ &+\frac{\varepsilon r_2^2}{\theta r_1}\left[\frac{1}{2}W_{20_1}\left(-\tau_1\right)\bar{c}e^{i\omega_0\tau_{2_0}}+W_{11_1}\left(-\tau_1\right)ce^{-i\omega_0\tau_{2_0}}\right]\\ &+\frac{\varepsilon r_2^2}{\theta r_1}\left[\frac{1}{2}W_{20_2}(-\tau_{2_0})e^{i\omega_0\tau_1}+W_{11_2}(-\tau_{2_0})e^{-i\omega_0\tau_1}\right]\\ &-\frac{\varepsilon r_2}{r_1}\left[\frac{1}{2}W_{20_2}(0)\bar{c}e^{i\omega_0\tau_{2_0}}+W_{11_2}(0)ce^{-i\omega_0\tau_{2_0}}\right.\\ &\left.+\ \frac{1}{2}W_{20_2}(-\tau_{2_0})\bar{c}+W_{11_2}(-\tau_{2_0})c\right].\end{aligned}\tag{3.13g}$$

Using this data and Theorem 5 given by [30] (see Section 3.2 in [30]), we can state the theorem that will give information about the properties of periodic solutions bifurcated from the equilibrium point $P^\star$ of the system (2.6) as:

Theorem 6 (*Properties Of Periodic Solutions*).

Assume that one of the conditions ***(H̃3-1), (H̃3-2)*** *or* ***(H̃4)*** *and the conditions* ***(H̃5), (H̃6)*** *given in Theorem 5 are satisfied. Then*

a. *Coefficient of the Poincaré normal form*

$$c_1(0)=\frac{i}{2\omega_0}\left(g_{20}(0)g_{11}(0)-2|g_{11}(0)|^2-\frac{1}{3}|g_{02}(0)|^2\right)+\frac{1}{2}g_{21}(0)\tag{3.14}$$

is calculated only by using the equations given in (3.13c) and (3.13d).

b. *There exist a $\epsilon_p>0$ such that for each $\epsilon\in(0,\epsilon_p)$ the system* (2.6) *has a periodic solution occurring at*

$$\tau_{2_0}+\mu(\epsilon)=\tau_{2_0}+\mu_2\epsilon^2+\mu_4\epsilon^4+h.o.t.$$

Assume that

(H̃7). $\mathrm{Re}(c_1(0))\neq 0$. *For ϵ small enough, the bifurcating periodic solutions exist after the bifurcation value $\tau_2=\tau_{2_0}$ if $\mu_2>0$; before the bifurcation value $\tau_2=\tau_{2_0}$ if $\mu_2<0$ where first non-zero coefficients in the Maclaurin expansions of bifurcation parameter $\mu=\tau-\tau_{2_0}$ is*

$$\mu_2=-\frac{\mathrm{Re}(c_1(0))}{\alpha_0'(\tau_{2_0})}.\tag{3.15}$$

c. *Bifurcating periodic solutions are unstable if* $\mathrm{Re}(c_1(0))>0$ *(Hopf bifurcation is subcritical); locally asymptotically stable if* $\mathrm{Re}(c_1(0))<0$ *(Hopf bifurcation is supercritical).*

d. *For $\epsilon\in(0,\epsilon_p)$ the period of the bifurcated periodic solution is*

$$T(\epsilon)=\frac{2\pi}{\omega_0}\left(1+T_2\epsilon^2+T_4\epsilon^4+h.o.t\right).$$

Hence for ϵ small enough, period is

$$T(\epsilon)\approx\frac{2\pi}{\omega_0}.\tag{3.16}$$

Moreover, the period increases if $T_2>0$; decreases if $T_2<0$ where

$$T_2=-\frac{\omega_0'(\tau_{2_0})\mu_2+\mathrm{Im}(c_1(0))}{\omega_0}.\tag{3.17}$$

Here, from equations (B.5) and (B.6) in Appendix B given by [30],

$$\alpha_0'(\tau_{2_0})=\omega_0\left(\frac{\mathrm{Re}(P)\,\mathrm{Re}(Q)+\mathrm{Im}(P)\,\mathrm{Im}(Q)}{(\mathrm{Re}(Q))^2+(\mathrm{Im}(Q))^2}\right)\tag{3.18a}$$

and

$$\omega_0'(\tau_{2_0})=\omega_0\left(\frac{\mathrm{Im}(P)\,\mathrm{Re}(Q)-\mathrm{Re}(P)\,\mathrm{Im}(Q)}{(\mathrm{Re}(Q))^2+(\mathrm{Im}(Q))^2}\right)\tag{3.18b}$$

where

$$\begin{aligned}P(\omega_0,\tau_{2_0})=&\left(R_{11}+R_{12}\cos(\tau_1^*\omega_0)+R_{13}\sin(\tau_1^*\omega_0)\right)\\ &+i\left(I_{11}+I_{12}\cos(\tau_1^*\omega_0)+I_{13}\sin(\tau_1^*\omega_0)\right),\\ Q(\omega_0,\tau_{2_0})=&\left(R_{21}+R_{22}\cos(\tau_1^*\omega_0)+R_{23}\sin(\tau_1^*\omega_0)\right)\\ &+i\left(I_{21}+I_{22}\cos(\tau_1^*\omega_0)+I_{23}\sin(\tau_1^*\omega_0)\right)\end{aligned}$$

in which

$$\begin{aligned}R_{11}=&r_1r_2^2\omega_0,\\ R_{12}=&d_1r_2n^4\left(d_1+2d_2\right)\omega_0-r_2\omega_0^3,\\ R_{13}=&d_1^2d_2r_2n^6-r_2n^2\left(2d_1+d_2\right)\omega_0^2,\\ R_{21}=&d_1r_1r_2^2n^2\left(\tau_{2_0}-\tau_1^*\right)-r_1r_2^2,\\ R_{22}=&d_1r_2n^4\left(d_1+d_2\right)-\left[r_2+r_2n^2\left(2d_1+d_2\right)\tau_{2_0}\right]\omega_0^2-d_1d_2r_2n^4+d_1^2d_2r_2n^6\tau_{2_0},\\ R_{23}=&r_2\tau_{2_0}\omega_0^3-d_1r_2n^4\left[\left(d_1+2d_2\right)\tau_{2,0}+2d_1r_2n^2\right]\omega_0,\\ I_{11}=&-d_1r_1r_2^2n^2,\\ I_{12}=&r_2n^2\left(2d_1+d_2\right)\omega_0^2-d_1^2d_2r_2n^6,\\ I_{13}=&d_1r_2n^4\left(d_1+2d_2\right)\omega_0-r_2\omega_0^3\\ I_{21}=&r_1r_2^2\left(\tau_{2,0}-\tau_1^*\right)\omega_0,\\ I_{22}=&\left(d_1r_2n^4\left(d_1+2d_2\right)\tau_{2,0}+2d_1r_2n^2\right)\omega_0-r_2\tau_{2_0}\omega_0^3,\\ I_{23}=&d_1r_2n^4\left(d_1+d_2\right)-\left(r_2+r_2n^2\left(2d_1+d_2\right)\tau_{2_0}\right)\omega_0^2-d_1d_2r_2n^4+d_1^2d_2r_2n^6\tau_{2_0}.\end{aligned}$$

4. Numerical simulations

The analytical results from the previous section will be validated by numerical simulations in this section. To analyze the impact of the diffusion term by comparing our results with the results of the analysis of the non-diffusive model done by Karaoğlu and Merdan [19], we use the same parameter values chosen in [19] given below:

$$r_1=0.45,\quad r_2=0.1,\quad \varepsilon=0.03,\quad \theta=0.05,\tag{4.1}$$

Most especially, the effect of the diffusion term and the effect of choice of τ_1 on the dynamics of the system (2.6) will be investigated.

The system (2.6) turns to the following system with these parameter values:

$$\begin{cases}\dfrac{\partial Y(x,t)}{\partial t}=d_1\dfrac{\partial^2Y(x,t)}{\partial x^2}+0.45Y(x,t)-0.03Y(x,t)Z(x,t),\\ \dfrac{\partial Z(x,t)}{\partial t}=d_2\dfrac{\partial^2Z(x,t)}{\partial x^2}+Z(x,t)\left(0.1-0.05\dfrac{Z(x,t-\tau_2)}{Y(x,t-\tau_1)}\right).\end{cases}\tag{4.2}$$

First of all, the case "$d_1=0$ and $d_2=0$" where diffusion and thus the random walk approach is ignored was analyzed by Karaoğlu and Merdan [19]. In this study, using the parameters specified by (4.1) and taking $d_1=0$ and $d_2=0$, they obtained the system next in line

$$\begin{cases}\dfrac{dY(t)}{dt}=0.45Y(t)-0.03Y(t)Z(t),\\ \dfrac{dZ(t)}{dt}=Z(t)\left(0.1-0.05\dfrac{Z(t-\tau_2)}{Y(t-\tau_1)}\right).\end{cases}\tag{4.3}$$

They applied their theoretical results we have talked about in Section 2 to this system. They concluded that the only positive equilibrium point of this system is $P^\star=(7.5,15)$ and it is locally asymptotically stable when $\tau_1\in[0,2.3034)$ and $\tau_2=0$; while it is unstable when $\tau_1>2.3034$ and $\tau_2=0$. In addition, they observed that if the delay term τ_1 is chosen from its stability interval $[0,2.3034)$ (which is calculated when $\tau_2=0$) as $\tau_1=2$, the equilibrium point $P^\star=(7.5,15)$ is locally asymptotically

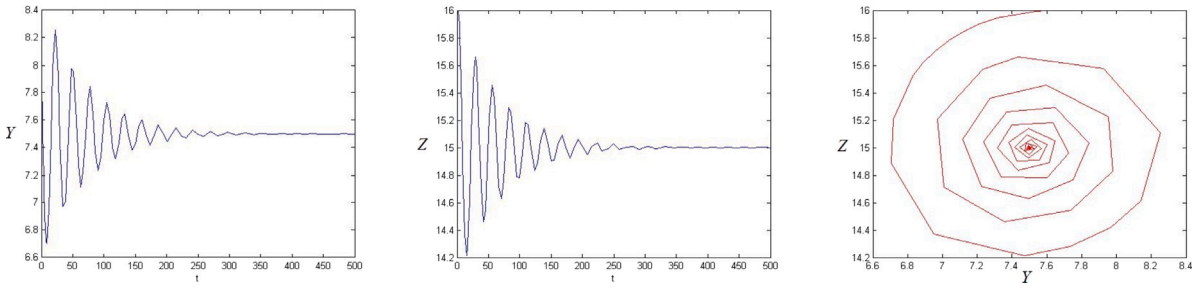

Fig. 1. Density versus time graph of prey (left), density versus time graph of predator (middle), and the phase portrait of the system (4.2) with zero diffusion (right). The initial conditions are $Y(0) = 8$ and $Z(0) = 16$. The delay values are $\tau_2 = 2$ and $\tau_1 = 1.5 \in [0, 2.3034)$. Simulations illustrate the asymptotic stability of the equilibrium point for $\tau_2 < \tau_{2_0} = 3.4582$ when $\tau_1 = 1.5$.

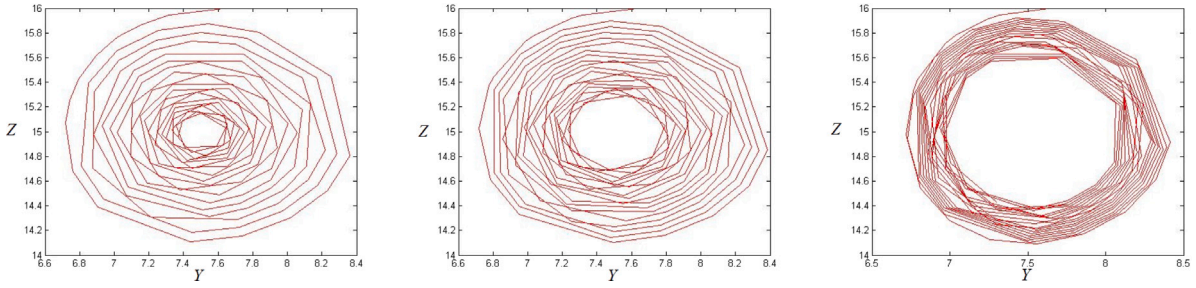

Fig. 2. The phase portraits of the system (4.2) with zero diffusion are shown, respectively, from left to right for $\tau_2 = 3.2$, $\tau_2 = 3.3$ and $\tau_2 = 3.4$. The initial conditions are $Y(0) = 8$ and $Z(0) = 16$. The delay value is $\tau_1 = 1.5 \in [0, 2.3034)$. Simulations show that the stability becomes nonlinear as τ_2 approaches $\tau_{2_0} = 3.4582$ when $\tau_1 = 1.5$.

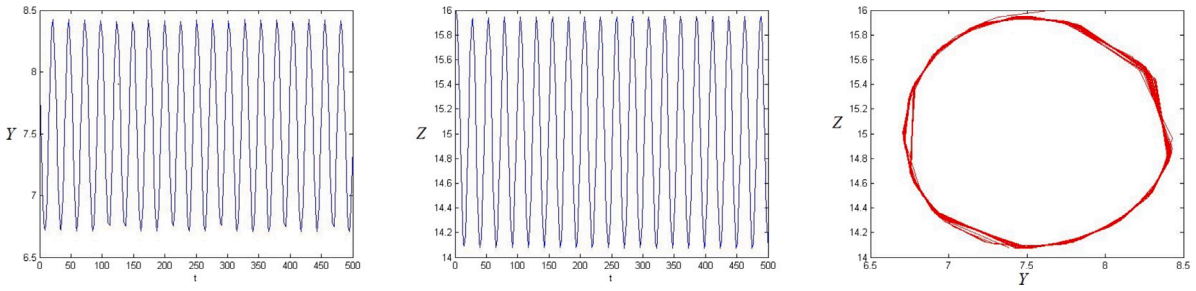

Fig. 3. Density versus time graph of prey (left), density versus time graph of predator (middle), and the phase portrait of the system (4.2) with zero diffusion (right). The initial conditions are $Y(0) = 8$ and $Z(0) = 16$. The delay values are $\tau_2 = 3.4582$ and $\tau_1 = 1.5 \in [0, 2.3034)$. From these simulations one can observe that as τ_2 passes through the critical value $\tau_2 = 3.4582$ a Hopf bifurcation arises at the equilibrium point $P^\star = (7.5, 15)$ when $\tau_1 = 1.5$.

stable when $\tau_2 \in [0, 2.2541)$; is unstable when $\tau_2 > 2.2541$, and Hopf bifurcation occurs in the system (4.3) when $\tau_2 = 2.2541$, that is, the system has a family of periodic solutions.

To obtain the theoretical results in Section 3.1 and Section 3.2, we used the algorithm developed by Bilazeroğlu and Merdan [30]. In this study, it was shown that if this algorithm is applied to the system (4.3), obtained results agree with the conclusions of the study done by Karaoğlu and Merdan [19] except for one difference. As in the study of Karaoğlu and Merdan [19], if τ_1 is chosen from its stability interval $[0, 2.3034)$ as $\tau_1 = 2$, then Eq. (3.9) has two distinct pairs of purely imaginary roots $\pm i\omega_{0_1} = \pm 0.1826i$ when $\tau_{2_{0,1}} = 2.7084$ and $\pm i\omega_{0_2} = \pm 0.2273i$ when $\tau_{2_{0,2}} = 2.2744$. The first delay value at which the pair of purely imaginary roots appears is $\tau_{2_{0,2}} = 2.2744$. If we round $\omega_{0_2} = 0.2273$ like $\omega_{0_2} = 0.23$ as it has been done by Karaoğlu and Merdan [19], we get $\tau_{2_0} = 2.2541$. Hence, results obtained by Bilazeroğlu and Merdan [30] keep up with those given by Karaoğlu and Merdan [19]. In the study of Bilazeroğlu and Merdan [30], it is also shown that Hopf bifurcation is supercritical, the bifurcating periodic solutions are stable and exist after the bifurcation value $\tau_{2_{0,2}} = 2.2744$. Moreover, it was investigated that in the neighborhood of bifurcation value period is ≈ 27.6431 and the period is increasing with respect to delay term τ_2.

In order to see the effect of the diffusion term on the population dynamic represented by the system (4.2), 6 different cases with different ecological meanings will be discussed:

(C1)	there is no diffusion, only time variation is considered
(C2)	the prey species moves randomly with a constant diffusion coefficient $d_2 = 0.05$ while the predator species does not move
(C3)	the predator species moves randomly with a constant diffusion coefficient $d_2 = 0.05$ while the prey species does not move
(C4)	the predator species moves randomly faster than the prey species
(C5)	prey and predator species move randomly with the same diffusion coefficient
(C6)	the prey species moves randomly faster than the predator species

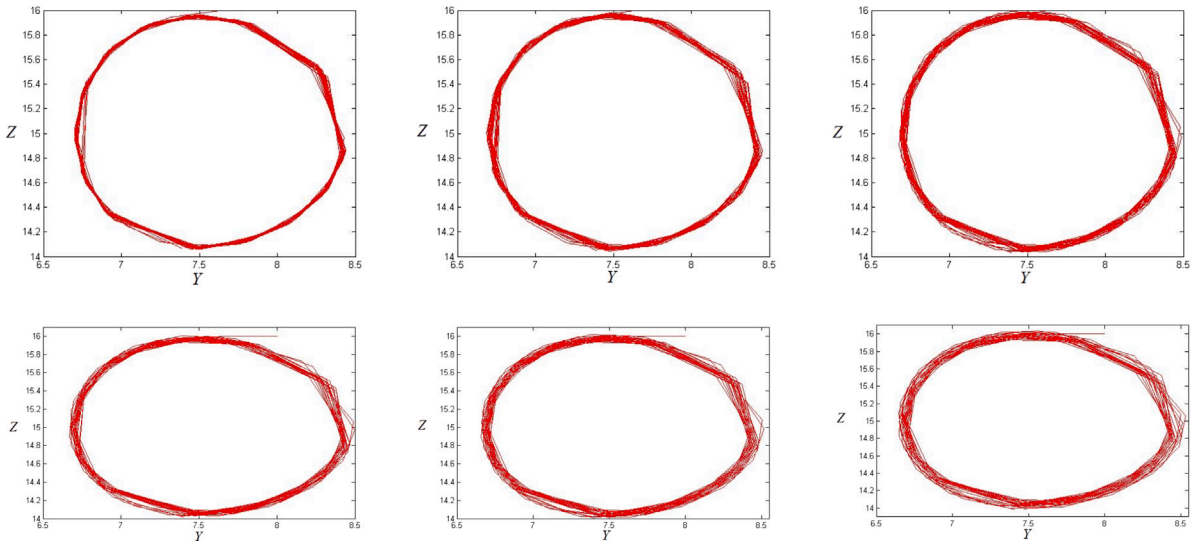

Fig. 4. The phase portraits of system (4.2) with zero diffusion are shown for the following delay values in the first row: $\tau_2 = 3.46$, $\tau_2 = 3.462$ and $\tau_2 = 3.464$, respectively, from left to right; and for the following delay values in the second row: $\tau_2 = 3.4626$, $\tau_2 = 3.4628$ and $\tau_2 = 3.47$, respectively, from left to right. The initial conditions are $Y(0) = 8$ and $Z(0) = 16$. The delay value is $\tau_1 = 1.5 \in [0, 2.3034)$. One can observe from the simulations that the bifurcating periodic solutions exist in a neighborhood of the critical bifurcation value $\tau_2 = 3.4582$ when $\tau_1 = 1.5$.

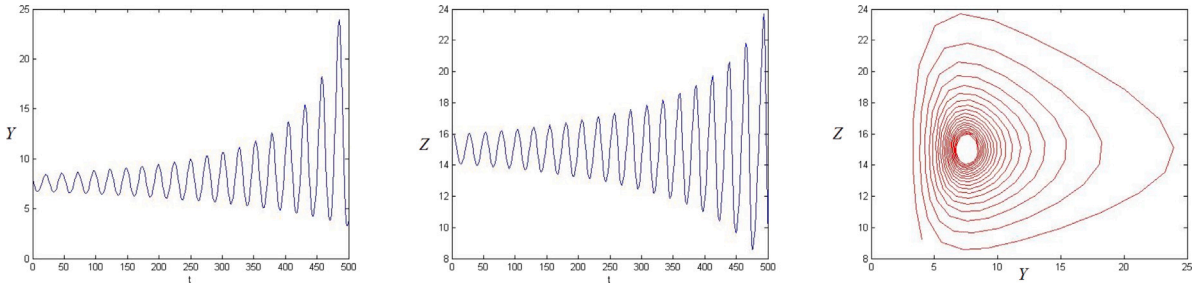

Fig. 5. Density versus time graph of prey (left), density versus time graph of predator (middle), and the phase portrait of the system (4.2) with zero diffusion (right). The initial conditions are $Y(0) = 8$ and $Z(0) = 16$. The delay values are $\tau_2 = 3.7$ and $\tau_1 = 1.5 \in [0, 2.3034)$. Simulations demonstrate the instability of the equilibrium point for $\tau_2 > \tau_{2_0} = 3.4582$ when $\tau_1 = 1.5$.

Table 2
Stability analysis and existence of Hopf bifurcation of system (4.2) when $\tau_2 = 0$.

	(C1)	(C2)	(C3)	(C4)	(C5)	(C6)
	$d_1 = 0$ $d_2 = 0$	$d_1 = 0.05$ $d_2 = 0$	$d_1 = 0$ $d_2 = 0.05$	$d_1 = 0.01$ $d_2 = 0.005$	$d_1 = 0.01$ $d_2 = 0.01$	$d_1 = 0.01$ $d_2 = 0.05$
ω_2	0.2007	0.1972	0.1874	0.1994	0.1982	0.1873
$\tau_{1_{2,0}}$	2.3034	3.6375	3.6005	2.6815	2.8097	3.8908
Stability Interval	$[0, 2.3034)$	$[0, 3.6375)$	$[0, 3.6005)$	$[0, 2.6815)$	$[0, 2.8097)$	$[0, 3.8908)$

Using the Corollaries 3–4 and Theorems 5–6 obtained in Section 3, the values required for existence analysis and directional analysis for those cases given in Table 2, Table 3 and Table 4.

We, first of all, discuss each case when $\tau_1 \neq 0$ and $\tau_2 = 0$. This means that a prey needs the time τ_1 to reach the maturity that the predator can hunt, while a predator has the ability to hunt as soon as it born. For all cases $S = -0.0020$, so the hypothesis **(H̃4)** $S < 0$ of Corollary 3 is satisfied. As a result, for each case, equilibrium point $(7.5, 15)$ is stable when $\tau_1 \in [0, \tau_{1_{2,0}})$ and $\tau_2 = 0$ where the associative $\tau_{1_{2,0}}$ can be found in third row of Table 2. Also, system (4.3) has a pair of purely imaginary eigenvalue $\pm i\omega_2$ when $\tau_1 = \tau_{1_{2,0}}$ and $\tau_2 = 0$. Moreover, system (4.3) undergoes a Hopf bifurcation as τ_1 passes through bifurcation value $\tau_{1_{2,0}}$ when $\tau_2 = 0$. Here, ω_2 and $\tau_{1_{2,0}}$ are calculated using the formulas (3.5) and (3.6a), respectively, for each case as given in Table 2.

From the ecological point of view, if the time required for prey to reach the maturity that the predator can hunt is less than $\tau_{1_{2,0}}$ and the initial adult population densities are close enough to the equilibrium point $(7.5, 15)$, then the solution of the system (4.2) will approach the equilibrium point $(7.5, 15)$ after some time. As a result, the long-term behavior of the solution will be predictable, and after a long enough time, the system's dynamic will not change. Nonetheless, if the time required for prey to reach the maturity that the predator can hunt is greater than but close enough to $\tau_{1_{2,0}}$ and the initial adult population densities are close enough to the equilibrium point $(7.5, 15)$, then the solution of the system (4.2) will approach the periodic solution. In this case, the long-term behavior of the solution will be still predictable, while there will be a dynamic that changes but repeats itself with a certain period. On the other hand, if the time that prey needs to mature

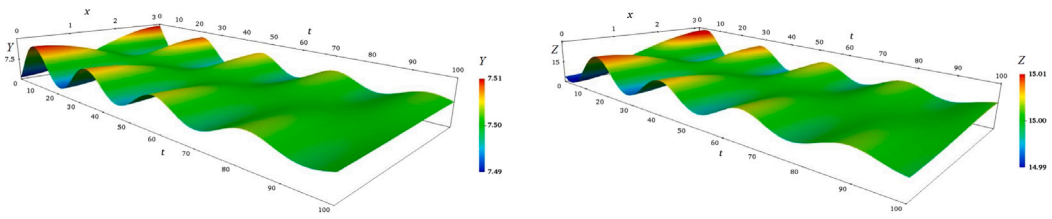

Fig. 6. Spatio-temporal graph of density of prey (left), spatio-temporal graph of density of predator (right). Here, diffusion coefficients are $d_1 = 0.05$ and $d_2 = 0$. The initial conditions are $Y(x,0) = 7.5 - 0.01\cos(x)$, $Z(x,0) = 15 - 0.01\cos(x)$. The delay values are $\tau_2 = 3.7$ and $\tau_1 = 1.5 \in [0, 3.6375)$. Simulations illustrate the asymptotic stability of the equilibrium point for $\tau_2 < \tau_{2_0} = 4.7057$ when $\tau_1 = 1.5$.

Table 3
Stability analysis and existence of Hopf bifurcation of system (4.2) when $\tau_1 = 1.5$ and $\tau_2 \neq 0$.

	(C1)	(C2)	(C3)	(C4)	(C5)	(C6)
	$d_1 = 0$ $d_2 = 0$	$d_1 = 0.05$ $d_2 = 0$	$d_1 = 0$ $d_2 = 0.05$	$d_1 = 0.01$ $d_2 = 0.005$	$d_1 = 0.01$ $d_2 = 0.01$	$d_1 = 0.01$ $d_2 = 0.05$
ω_0	0.2459	0.2604	0.2593	0.2522	0.2539	0.2611
τ_{2_0}	3.4582	4.7057	5.4452	3.9557	4.1562	5.6476
Stability Interval	$[0, 3.4582)$	$[0, 4.7057)$	$[0, 5.4452)$	$[0, 3.9557)$	$[0, 4.1562)$	$[0, 5.6476)$
$\alpha_0'(\tau_{2_0})$	0.0131	0.0155	0.0149	0.0138	0.0153	0.0143

is larger enough than $\tau_{1_{2,0}}$ the equilibrium point $(7.5, 15)$ is unstable, and stable periodic solutions do not exist anymore. As a result, the long-term behavior of the solution will be unpredictable.

Now, we argue the each of these 6 cases as $\tau_1 = 1.5$ and $\tau_2 \neq 0$. In other words, we consider that a prey needs the time $\tau_1 = 1.5$ to reach the maturity that predator can hunt and the time required for the predator to have the ability to hunt is τ_2.

For undertaken 6 different cases, from Corollary 4 and Theorem 5, Table 3 shows that the equilibrium point $P^\star = (7.5, 15)$ of the system (4.2) is locally asymptotically stable when $\tau_1 = 1.5$ and $\tau_2 \in [0, \tau_{2_0})$ (see Fifth line of Table 3). It is also indicated in this table that because the characteristic equation of the system (4.2) has a pair of purely imaginary roots $\pm i\omega_0$ when $\tau_1 = 1.5$ and $\tau_2 = \tau_{2_0}$, the equilibrium point $P^\star = (7.5, 15)$ lose its stability and becomes unstable when $\tau_1 = 1.5$ and $\tau_2 > \tau_{2,0}$. Moreover, since transversality condition holds (see Last line of Table 3), Hopf bifurcation occurs in the system (4.2) as τ_2 passes through bifurcation value τ_{2_0} when $\tau_1 = 1.5$. That is, according to Theorem 5 for each diffusion coefficient value pair given in Table 3, the system (4.2) has a family of periodic solutions in a neighborhood of τ_{2_0} while $\tau_1 = 1.5$.

The condition **(H̃5)** is not satisfied in any case, but using MATLAB it is shown that system (4.3) has two pairs of purely imaginary eigenvalues $\pm i\omega_{0_1}$ when $\tau_2 = \tau_{2_{0_1}}$ and $\pm i\omega_{0_2}$ when $\tau_2 = \tau_{2_{0_2}}$. Choosing the smallest τ_2 as τ_{2_0} and the corresponding eigenvalue as $\pm i\omega_0$ we obtain the values given in Table 3. Also, in each case, we used the formula (3.18a) to specify $\alpha_0'(\tau_{2_0})$.

According to Theorem 6, Table 4 gives the following information about the properties of existing Hopf bifurcation and bifurcating periodic solutions for all cases as: (i) since $\mathrm{Re}(c_1(0)) < 0$, Hopf bifurcation is supercritical and the resulting periodic solutions are stable; (ii) because $\mu_2 > 0$, bifurcating periodic solutions occur after the bifurcation value τ_{2_0}; (iii) the period of the periodic solutions is as given in the last line of Table 4 when the value of τ_2 is close enough to the bifurcation value τ_{2_0} and the period increases with respect to τ_2 since $T_2 > 0$. Here, in each case, we used the formulas (3.14), (3.15), (3.16) and (3.17) to calculate $\mathrm{Re}(c_1(0)) < 0$, $\mu_2 > 0$, period and $T_2 > 0$, respectively.

To support these theoretical results, for each case, we perform some numerical simulations using the technique described as follows: For Figs. 1–5, MATLAB DDE (Delay Differential Equations) solver is used to simulate the system. For Figs. 6–33, the coupled initial boundary-value problem, defined in (2.6), have been analyzed within the one-dimensional spatial domain $\mathcal{B} := [0, \pi]$ and the time interval $\mathcal{T} := [0, t_{\mathrm{sim}}]$ where $t_{\mathrm{sim}} \in \{100, 200\}$ denotes the total simulation time. The transient partial differential Eq. (2.6) has been discretized spatially through the finite element method using two-node linear line elements and, in time, using the Crank–Nicolson scheme. The discretized coupled predator–prey problem has been implemented into a general-purpose finite element program FEAP [32] through the newly developed problem-specific user codes furnished with an efficient tool for memory management to handle the history of delay variables. It is worth noting that the resultant coupled system of nonlinear equations has been solved monolithically using the iterative Newton-type solver at each time step. In the numerical analyses of all the simulations depicted in Figs. 6–33, the element size h and the value of time step Δt are chosen $h = \pi/100$ and $\Delta t = 10^{-3}$, respectively. In other words, the finite element analysis has been conducted using 100 elements in either 10^5 or $2 \cdot 10^5$ time steps. Moreover, flux-free (homogeneous Neumann) boundary conditions $\partial Y(x,t)/\partial x = \partial Z(x,t)/\partial x = 0$ for all $x \in \partial\mathcal{B} := \{0, \pi\}$ and $t \in \mathcal{T} := [0, t_{\mathrm{sim}}]$ have been adopted. The initial values of the field variables are chosen to be $(Y_0(x), Z_0(x)) = (7.5 - 0.01\cos(x), 015 - 0.01\cos(x))$.

Simulations labeled by figures in the third row of Table 5 show that the equilibrium point is asymptotically stable for a chosen τ_2 less than the corresponding τ_{2_0} for each case in turn. In Figures, shown in the fourth row of Table 5, it is represented that a Hopf bifurcation arises at $P^\star = (7.5, 15)$ when τ_2 passes through associated critical value τ_{2_0} for all cases respectively. Simulations denoted in figures in the fifth row of Table 5 demonstrate that the equilibrium point $P^\star = (7.5, 15)$ is unstable for a chosen τ_2 greater than the corresponding τ_{2_0} for the apiece case in turn. In all simulations, τ_1 is selected from the stability interval as $\tau_1 = 1.5$ and τ_{2_0} is given in Table 3 for every case, respectively.

Now, we will interpret these theoretical results from the ecological point of view. If a prey needs the time $\tau_1 = 1.5$ to reach the maturity that predator can hunt, and the time τ_2 required for the predator to have the ability to hunt is less than τ_{2_0}, and the initial adult population densities are close enough to the equilibrium point $(7.5, 15)$, then the solution of the system (4.2) will approach the equilibrium point $(7.5, 15)$ after some time. Consequently, the long-term behavior of the solution will be predictable and after a long enough time the dynamic of the

Table 4
Direction analysis of Hopf bifurcation of system (4.2) when $\tau_1^* = 1.5$ and $\tau_2 \neq 0$.

	(C1)	(C2)	(C3)	(C4)	(C5)	(C6)
	$d_1 = 0$ $d_2 = 0$	$d_1 = 0.05$ $d_2 = 0$	$d_1 = 0$ $d_2 = 0.05$	$d_1 = 0.01$ $d_2 = 0.005$	$d_1 = 0.01$ $d_2 = 0.01$	$d_1 = 0.01$ $d_2 = 0.05$
$\mathrm{Re}(c_1(0))$	−0.0009	−0.0023	−0.0030	−0.0013	−0.0016	−0.0032
μ_2	0.0651	0.1470	0.2035	0.0895	0.1025	0.2243
Period	25.5554	24.1296	24.2300	24.9147	24.7483	24.0633
T_2	0.0324	0.0410	0.0356	0.0346	0.0349	0.0368

Table 5
Numerical simulations of system (4.2) when $\tau_1 = 1.5$ and $\tau_2 \neq 0$.

	(C1)	(C2)	(C3)	(C4)	(C5)	(C6)
	$d_1 = 0$ $d_2 = 0$	$d_1 = 0.05$ $d_2 = 0$	$d_1 = 0$ $d_2 = 0.05$	$d_1 = 0.01$ $d_2 = 0.005$	$d_1 = 0.01$ $d_2 = 0.01$	$d_1 = 0.01$ $d_2 = 0.05$
(7.5,15) is Stable	Fig. 1	Fig. 6	Fig. 9	Fig. 13	Fig. 17	Fig. 21
Periodic Solution	Fig. 3	Fig. 7	Fig. 11	Fig. 14	Fig. 19	Fig. 23
(7.5,15) is Unstable	Fig. 5	Fig. 8	Fig. 12	Fig. 16	Fig. 20	Fig. 24

Table 6
Effects of diffusion in system (4.2) when $\tau_1 = 1.5$ and $\tau_2 \neq 0$.

	Effects	Compared Cases
(E1)	Effect of existence of diffusion	(C1) and (C5)
(E2)	Effect of the diffusion term d_1	(C3) and (C6)
(E3)	Effect of the diffusion term d_2	(C4) and (C5) (C5) and (C6)
(E4)	Effect of increase in diffusion terms (at least one of them is zero)	(C1) and (C2), (C2) and (C3)
(E5)	Effect of increase in diffusion terms (at least one of them is zero)	(C4) and (C5), (C5) and (C6)

system will not change. At the same time, if the time required for a predator to have the ability to hunt is larger than but close enough to τ_{2_0} and the initial conditions are close enough to the equilibrium point $(7.5, 15)$, then the solution of the system (4.2) will approach the periodic solution. In this case, the long-term behavior of the solution will be still predictable, while there will be an oscillating dynamic that changes but repeats itself with a certain period of time. On the other hand, if the time required for a predator to have the ability to hunt is larger enough than τ_{2_0}, the equilibrium point $(7.5, 15)$ is unstable, and stable periodic solutions do not exist anymore. As a result, the long-term behavior of the solution will be unpredictable.

We have concluded from the theoretical studies that occurring Hopf bifurcations are all supercritical. In the dynamics of supercritical Hopf bifurcation, a locally asymptotically stable equilibrium point loses its stability at a critical value of the parameter, and just before it loses this stability, the equilibrium point becomes nonlinearly stable. One can see from the simulations in Fig. 2 that the phase portraits of the system (4.2) with zero diffusion for $\tau_2 = 3.2$, $\tau_2 = 3.3$ and $\tau_2 = 3.4$, respectively, from left to right. Simulations represent that the stability becomes nonlinear as τ_2 increases and approaches the critical value $\tau_{2_0} = 3.4582$ when $\tau_1 = 1.5$ for **(C1)**. Moreover, Fig. 10, Fig. 18, and Fig. 22 show that the equilibrium point $P^\star = (7.5, 15)$ is nonlinearly asymptotically stable for a chosen τ_2 less than but very close to the corresponding τ_{2_0} for the cases **(C3)**, **(C5)** and **(C6)**, respectively. These results support the predicted theoretical result.

In contrast, in the dynamics of supercritical Hopf bifurcation, when a locally asymptotically stable equilibrium point loses its stability at a critical value of the parameter, stable periodic solutions arise at and after the critical value of the parameter. Also, they exist on the right half part of an interval containing the critical value of the parameter. In Fig. 4, simulations represent that the bifurcating periodic solutions exist in a neighborhood of the critical value $\tau_2 = 3.4582$ when $\tau_1 = 1.5$ for **(C1)**. Additionally, because of the smoothness in the dynamic of the Hopf bifurcation, we expect that the instability of the equilibrium solution after the critical value is nonlinear first of all. Simulations in Fig. 15 represents that the equilibrium point $P^\star = (7.5, 15)$ is nonlinearly unstable for $\tau_2 > \tau_{2_0} = 3.9557$ when $\tau_1 = 1.5$ for **(C4)**.

Using the obtained numerical results given in Table 3 and Table 4; and simulations given in Figs. 1–24, we want to analyze the following five different effects of random walk: **(E1)** Impact of random walk of both species (Effect of the existence of diffusion), **(E2)** Impact of random walk of the prey species (Effect of the diffusion term d_1), **(E3)** Impact of random walk of the predator species (Effect of the diffusion term d_2) **(E4)**, Impact of increase in movement rate of one species (Effect of diffusion when at least one of the diffusion terms is zero), and **(E5)** Impact of increase in movement rate of two species (Effect of increase in diffusion when both of the diffusion terms are non-zero). We fix the maturation period for predator as $\tau_1 = 1.5$ and compare the respective cases as given in Table 6 to analyze these effects.

First of all, to analyze the effect of the existence of diffusion, we compare **(C1)** (diffusive terms are both zero) and **(C5)** (nonzero diffusion terms have the same value of 0.01). If the diffusion terms are added to the system, the equilibrium point remains even if it takes longer

Table 7
Change in stability interval of the equilibrium point and period of the periodic solutions of system (4.2) when $\tau_1 = 1.5$.

	(E1)		(E2)	
	(C1)	(C5)	(C3)	(C6)
	$d_1 = 0$ $d_2 = 0$	$d_1 = 0.01$ $d_2 = 0.01$	$d_1 = 0$ $d_2 = 0.05$	$d_1 = 0.01$ $d_2 = 0.05$
Stability Interval	$[0, 3.4582)$	$[0, 4.1562)$	$[0, 5.4452)$	$[0, 5.6476)$
Numerical Simulations	when $\tau_2 = 3.7$		when $\tau_2 = 5.5$	
	unstable Fig. 5	stable Fig. 17	unstable Fig. 12	stable Fig. 22
Period	decreases		decreases	
	25.5554	24.7483	24.2300	24.0633
	(E3)			
	(C4)	(C5)	(C5)	(C6)
	$d_1 = 0.01$ $d_2 = 0.005$	$d_1 = 0.01$ $d_2 = 0.01$	$d_1 = 0.01$ $d_2 = 0.01$	$d_1 = 0.01$ $d_2 = 0.05$
Stability Interval	$[0, 3.9557)$	$[0, 4.1562)$	$[0, 4.1562)$	$[0, 5.6476)$
Numerical Simulations	when $\tau_2 = 4.05$		when $\tau_2 = 5.5$	
	unstable Fig. 15	stable Fig. 18	unstable Fig. 20	stable Fig. 22
Period	decreases		decreases	
	24.9147	24.7483	24.7483	24.0633
	(E4)			
	(C1)	(C2)	(C2)	(C3)
	$d_1 = 0$ $d_2 = 0$	$d_1 = 0.05$ $d_2 = 0$	$d_1 = 0.05$ $d_2 = 0$	$d_1 = 0$ $d_2 = 0.05$
Stability Interval	$[0, 3.4582)$	$[0, 4.7057)$	$[0, 4.7057)$	$[0, 5.4452)$
Numerical Simulations	when $\tau_2 = 3.7$		when $\tau_2 = 5$	
	unstable Fig. 5	stable Fig. 6	unstable Fig. 8	stable Fig. 10
Period	decreases		decreases	
	25.5554	24.1296	24.1296	24.2300
	(E5)			
	(C4)	(C5)	(C5)	(C6)
	$d_1 = 0.01$ $d_2 = 0.005$	$d_1 = 0.01$ $d_2 = 0.01$	$d_1 = 0.01$ $d_2 = 0.01$	$d_1 = 0.01$ $d_2 = 0.05$
Stability Interval	$[0, 3.9557)$	$[0, 4.1562)$	$[0, 4.1562)$	$[0, 5.6476)$
Numerical Simulations	when $\tau_2 = 4.05$		when $\tau_2 = 5.5$	
	unstable Fig. 15	stable Fig. 18	unstable Fig. 20	stable Fig. 22
Period	decreases		decreases	
	24.9147	24.7483	24.7483	24.0633

for the predator to have the ability to hunt. The equilibrium point $P^\star = (7.5, 15)$ is asymptotically stable when $\tau_2 \in [0, 3.4582)$ if there is no diffusion. Besides, it is asymptotically stable when $\tau_2 \in [0, 4.1562)$ if the prey species and the predator species move randomly with a same constant diffusion coefficient $d_1 = d_2 = 0.01$ (see Table 3 and Table 7). If we fixed $\tau_1 = 1.5$ and $\tau_2 = 3.7$ it is seen that the equilibrium point $P^\star = (7.5, 15)$ is unstable in Fig. 5 since $\tau_2 = 3.7 > 3.4582$. However, because $3.7 \in [0, 4.1562)$, Fig. 17 represents that the equilibrium point $P^\star = (7.5, 15)$ is asymptotically stable for **(C5)**. On the other hand, in a more realistic model (the diffusive model in **(C5)**), periodic solutions occur in a higher time (τ_2) required for the predator to have the ability to hunt. The periodic solution emerges when $\tau = 3.4582$ (see Fig. 3) in **(C1)**, while it arises when $\tau = 4.1560$ (see Fig. 19) in **(C5)**. As a final effect, if diffusion is taken into consideration, the period of the periodic solutions decreases (see Table 4).

Table 8
Stability analysis and existence of Hopf bifurcation of system (4.2) when $d_1 = 0.01$ and $d_2 = 0.005$.

	(D1)	(D2)	(D3)
	$\tau_1 = 0.5$	$\tau_1 = 1.5$	$\tau_1 = 2$
ω_0	0.2670	0.2522	0.2381
τ_{2_0}	5.4642	3.9557	3.0709
Stability Interval	$[0, 5.4642)$	$[0, 3.9557)$	$[0, 3.0709)$
$\alpha_0'(\tau_{2_0})$	0.0154	0.0149	0.0109

Table 9
Direction analysis of Hopf bifurcation in system (4.2) when $d_1 = 0.01$ and $d_2 = 0.005$.

	(D1)	(D2)	(D3)
	$\tau_1 = 0.5$	$\tau_1 = 1.5$	$\tau_1 = 2$
$\mathrm{Re}(c_1(0))$	−0.0019	−0.0013	−0.0011
μ_2	0.1248	0.0895	0.1044
Period	23.5314	24.9147	26.3902
T_2	0.0447	0.0346	0.0264

As we did in the first effect, we compare respective cases as given in Table 6 to analyze the other effects. We observe that whatever the effect **(E1–E5)** we analyze, we have obtained similar changes in the dynamics of the system (4.2) when the maturation period for a predator is fixed as $\tau_1 = 1.5$. If we add diffusion term to the system **(E1)** or if we increase the value of one or both of the diffusion coefficients **(E2–E5)**, we observe the following changes in the dynamics of the system (4.2) as summarized in the Table 7:

1. The equilibrium point remains stable for a more extended period according to the predator's ability to hunt (τ_2).

2. Periodic solutions occur in a higher time (τ_2) required for the predator to have the ability to hunt.

3. The period of the periodic solutions decreases, that is to say, the system repeats itself in a shorter time.

These ecologically means that if the time required for prey to reach maturity is fixed as $\tau_1 = 1.5$ in the stability interval, then the predator needs to gain the ability to hunt later so that the dynamic can repeat itself. And this repetition, which means continuing to live together, occurs over a shorter period.

In order to investigate the effect of the time required for the prey species to reach maturity (τ_1) on the population dynamics represented by the system (4.2), the diffusion coefficient values are fixed as $d_1 = 0.01$ and $d_2 = 0.005$ **((C4))**. One can see from Table 2 that the equilibrium point is locally asymptotically stable if $\tau_1 \in [0, 2.6815)$ when $\tau_2 = 0$. Because of this, to analyze the effect of τ_1, we choose values in this stability interval as **(D1)**: $\tau_1 = 0.5$, **(D2)**: $\tau_1 = 1.5$, and **(D3)**: $\tau_1 = 2$.

Table 8 shows that the equilibrium point $P^\star = (7.5.15)$ of the system (4.2) is locally asymptotically stable if $\tau_2 \in [0, 5.4642)$ when $\tau_1 = 0.5$; if $\tau_2 \in [0, 3.9557)$ when $\tau_1 = 1.5$ and if $\tau_2 \in [0, 3.0709)$ when $\tau_1 = 2$ (see Fifth line of Table 8). Moreover, the equilibrium point $P^\star = (7.5, 15)$ loses its stability, and Hopf bifurcation occurs in the system at the delay value $\tau_2 = \tau_{2_0}$, since the characteristic equation of the system $\pm i\omega_0$ has just a pair of purely imaginary root. Also, the equilibrium point $P^\star = (7.5.15)$ is unstable if $\tau_2 > 5.4642$ when $\tau_1 = 0.5$; if $\tau_2 > 3.9557$ when $\tau_1 = 1.5$ and if $\tau_2 > 3.0709$ when $\tau_1 = 2$. This means that, the system (4.2) has a family of periodic solutions in a neighborhood of τ_{2_0} by Theorem 5.

Table 9 gives the following information about the properties of the occurring Hopf bifurcation in the system (4.2) for all cases **(D1)**-**(D3)** according to Theorem 6: since $\mathrm{Re}(c_1(0)) < 0$, Hopf bifurcation

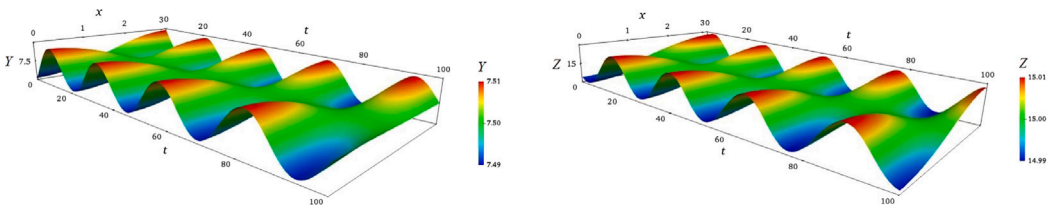

Fig. 7. Spatio-temporal graph of density of prey (left), spatio-temporal graph of density of predator (right). Here, diffusion coefficients are $d_1 = 0.05$ and $d_2 = 0$. The initial conditions are $Y(x,0) = 7.5 - 0.01\cos(x)$, $Z(x,0) = 15 - 0.01\cos(x)$. The delay values are $\tau_2 = 4.7057$ and $\tau_1 = 1.5 \in [0, 3.6375)$. From these simulations one can observe that as τ_2 passes through the critical value $\tau_2 = 4.7057$ a Hopf bifurcation arises at the equilibrium point $P^\star = (7.5, 15)$ when $\tau_1 = 1.5$.

Table 10
Numerical simulations of system (4.2) when $d_1 = 0.01$ and $d_2 = 0.005$.

	(D1)	(D2)	(D3)
	$\tau_1 = 0.5$	$\tau_1 = 1.5$	$\tau_1 = 2$
(7.5,15) is Stable	Fig. 25	Fig. 28	Fig. 31
Periodic Solution	Fig. 26	Fig. 29	Fig. 32
(7.5,15) is Unstable	Fig. 27	Fig. 30	Fig. 33

is supercritical and the resulting periodic solutions are stable; because $\mu_2 > 0$, bifurcating periodic solutions occur after the bifurcation value τ_{2_0}. Moreover, the period of the periodic solutions is as in the last line of Table 9 when τ_2 is close enough to the bifurcation value τ_{2_0}. Also, since $T_2 > 0$, this period increases as the bifurcation parameter τ_2 moves away from the bifurcation value τ_{2_0}.

To support these theoretical results, we simulate the system (4.2) for each case. One can see for each case in turn that the equilibrium point is asymptotically stable for a chosen τ_2 less than the corresponding τ_{2_0} from the simulations labeled by figures in the third row of Table 10. Simulations denoted in figures in the fourth row of Table 10 demonstrate that a Hopf bifurcation arises at $P^\star = (7.5, 15)$ when τ_2 passes through associated critical value τ_{2_0} for all cases respectively. In Figures, shown in the last row of Table 10, it is represented that the equilibrium point $P^\star = (7.5, 15)$ is unstable for a chosen τ_2 greater than the corresponding τ_{2_0} for the apiece case in turn. In all simulations, diffusion coefficients are fixed as $d_1 = 0.01$ and $d_2 = 0.005$. If we increase the value of τ_1 when $d_1 = 0.01$ and $d_2 = 0.005$, the following changes in the dynamics of the system (4.2) are observed:

1. The equilibrium point remains stable for a more shorter period according to the predator's ability to hunt (τ_2) (see Fifth row of Table 8).

2. Periodic solutions occur at an earlier time (τ_2) required for the predator to be capable of hunting (see Fourth row of Table 8).

3. The period of the periodic solutions increases (see Last row of Table 9).

These ecologically means that, if the prey and predator species moves randomly with a constant diffusion coefficients $d_1 = 0.01$ and $d_1 = 0.005$, respectively, when the prey needs longer time to mature, the predator needs to gain the ability to hunt earlier so that the dynamic can repeat itself. And this repetition, which means living together, occurs over a more extended period.

5. Conclusion

Mathematical modeling and its analysis have been often used to understand, explain and offer solutions to real life problems. Reaction–diffusion mechanism and delay in response to inputs or stimuli inherent in many problems. So, while modeling a real life problem, not neglecting reaction–diffusion mechanism and delay term will provide a more realistic representation of the problem [30].

In this study, we take into account a diffusive ratio-dependent predator–prey model (2.6) involving two discrete delays under the Neumann boundary conditions. These delay parameters represent the time required for prey to reach the maturity that the predator can hunt, say τ_1, and the time needed for the predator to develop hunting skills, say τ_2. Our first question is what changes will occur in the qualitative behavior of the system as these delay parameters vary.

Hopf bifurcation is a type of bifurcation in which the stability structure of the equilibrium point of the system changes as a parameter in the system varies. This change is attended by the emergence or vanish of periodic solutions while a parameter in the system varies in an interval. The presence of periodic behaviors in the dynamics of a predator–prey system represents coexistence, continuing to live together.

First of all, we assumed that the predator species can predate as soon as they are born, $\tau_2 = 0$, and they only catch mature adult prey with a certain maturation time; in other words, the prey must be old enough to be caught. We observed that if the other parameters in the model satisfy one of the conditions given in Corollary 2, then the equilibrium point $P^\star$ is absolutely stable; that is, the Hopf bifurcation never occurs in the system (2.6) when $\tau_2 = 0$. Moreover, if the other parameters in the model satisfy the condition given in Corollary 3, then the system (2.6) has a family of periodic solutions in a neighborhood of critical bifurcation value $\tau_{1_{2,0}}$ when $\tau_2 = 0$.

Secondly, we assumed that the time required for prey to reach the maturity that the predator can hunt, τ_1, is nonzero and is fixed in the stability interval to guarantee that the positive equilibrium point is stable when $\tau_2 = 0$. Additionally, we presumed that some predators take some time to develop the ability to hunt; in other words, the predator must reach adulthood before it can successfully catch prey. Next, we chose the delay parameter, τ_2, which represents the time the predator needs to gain the ability to hunt as the bifurcation parameter. In this case, we obtained that under the conditions given in Theorem 5, the (2.6) undergoes a Hopf bifurcation at the equilibrium point $P^\star$, that is to say, a family of periodic solutions appears out of the equilibrium point $P^\star$ as the delay parameter τ_2 passes through τ_{2_0}. We have determined these results using the algorithm in [30] one again. Using the same algorithm, some of the bifurcation properties, such as stability, direction, and also period are investigated. In order to support these theoretical results and to answer our second question, we analyzed a model with constant coefficients, the system (4.2), and performed some numerical simulations to support the analytical results.

To see the effect of the diffusion term on the population dynamic represented by the system (4.2), six different situations with different ecological meanings were discussed. The following changes have been observed in the dynamics of the system (4.2): (i) the equilibrium point remains stable for a more extended period according to the predator's ability to hunt (τ_2), (ii) periodic solutions occur in a higher time (τ_2) required for the predator to have the ability to hunt, and (iii) the period of the periodic solutions decreases, which means that the system repeats itself in a shorter time. These ecologically means that if the time required for prey to reach maturity is fixed as $\tau_1 = 1.5$ in the stability interval, then the predator needs to gain the ability to hunt later so

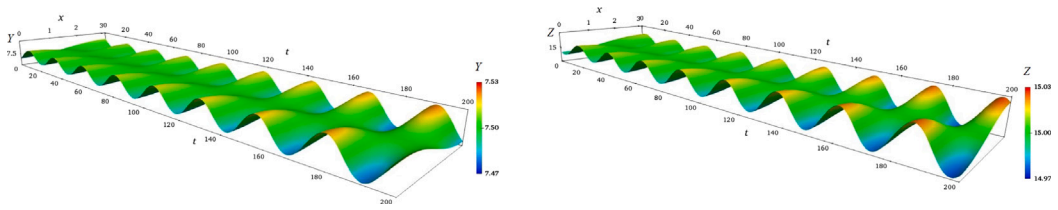

Fig. 8. Spatio-temporal graph of density of prey (left), spatio-temporal graph of density of predator (right). Here, diffusion coefficients are $d_1 = 0.05$ and $d_2 = 0$. The initial conditions are $Y(x,0) = 7.5 - 0.01\cos(x)$, $Z(x,0) = 15 - 0.01\cos(x)$. The delay values are $\tau_2 = 5$ and $\tau_1 = 1.5 \in [0, 3.6375)$. Simulations demonstrate the instability of the equilibrium point for $\tau_2 > \tau_{2_0} = 4.7057$ when $\tau_1 = 1.5$.

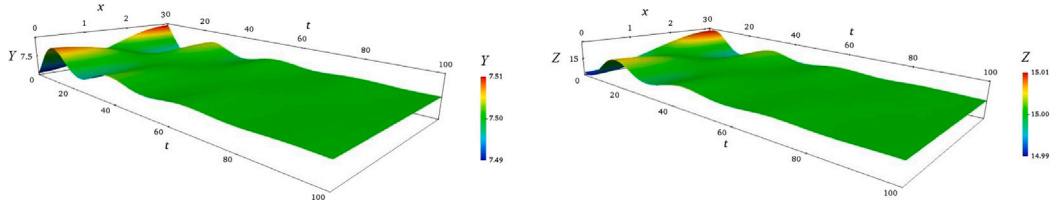

Fig. 9. Spatio-temporal graph of density of prey (left), spatio-temporal graph of density of predator (right). Here, diffusion coefficients are $d_1 = 0$ and $d_2 = 0.05$. The initial conditions are $Y(x,0) = 7.5 - 0.01\cos(x)$, $Z(x,0) = 15 - 0.01\cos(x)$. The delay values are $\tau_2 = 2$ and $\tau_1 = 1.5 \in [0, 3.6005)$. Simulations illustrate the asymptotic stability of the equilibrium point for $\tau_2 < \tau_{2_0} = 5.4452$ when $\tau_1 = 1.5$.

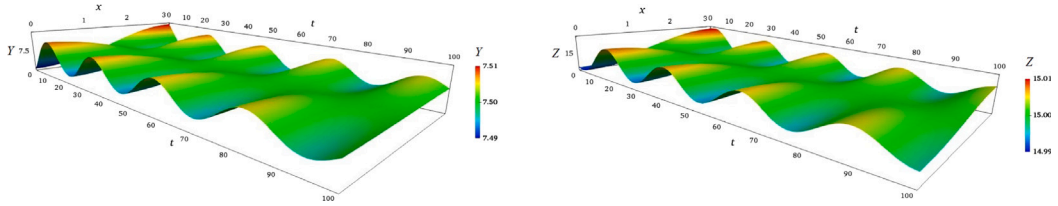

Fig. 10. Spatio-temporal graph of density of prey (left), spatio-temporal graph of density of predator (right). Here, diffusion coefficients are $d_1 = 0$ and $d_2 = 0.05$. The initial conditions are $Y(x,0) = 7.5 - 0.01\cos(x)$, $Z(x,0) = 15 - 0.01\cos(x)$. The delay values are $\tau_2 = 5$ and $\tau_1 = 1.5 \in [0, 3.6005)$. Simulations illustrate the nonlinearly asymptotic stability of the equilibrium point for $\tau_2 < \tau_{2_0} = 5.4452$ when $\tau_1 = 1.5$.

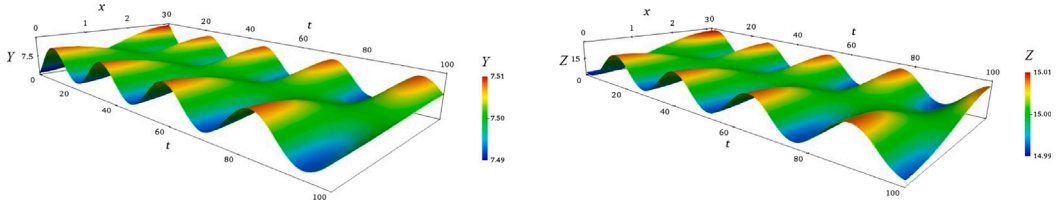

Fig. 11. Spatio-temporal graph of density of prey (left), spatio-temporal graph of density of predator (right). Here, diffusion coefficients are $d_1 = 0$ and $d_2 = 0.05$. The initial conditions are $Y(x,0) = 7.5 - 0.01\cos(x)$, $Z(x,0) = 15 - 0.01\cos(x)$. The delay values are $\tau_2 = 5.4450$ and $\tau_1 = 1.5 \in [0, 3.6005)$. From these simulations one can observe that as τ_2 passes through the critical value $\tau_2 \approx 5.4452$ a Hopf bifurcation arises at the equilibrium point $P^\star = (7.5, 15)$ when $\tau_1 = 1.5$.

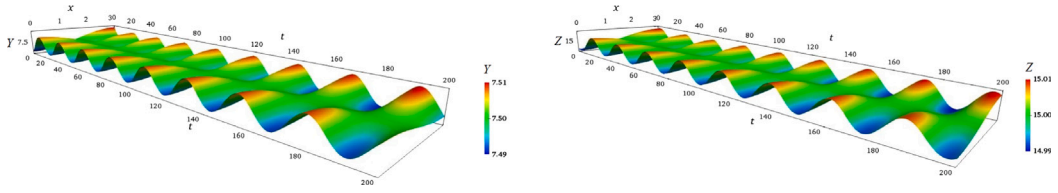

Fig. 12. Spatio-temporal graph of density of prey (left), spatio-temporal graph of density of predator (right). Here, diffusion coefficients are $d_1 = 0$ and $d_2 = 0.05$. The initial conditions are $Y(x,0) = 7.5 - 0.01\cos(x)$, $Z(x,0) = 15 - 0.01\cos(x)$. The delay values are $\tau_2 = 5.5$ and $\tau_1 = 1.5 \in [0, 3.6005)$. Simulations demonstrate the instability of the equilibrium point for $\tau_2 > \tau_{2_0} = 5.4452$ when $\tau_1 = 1.5$.

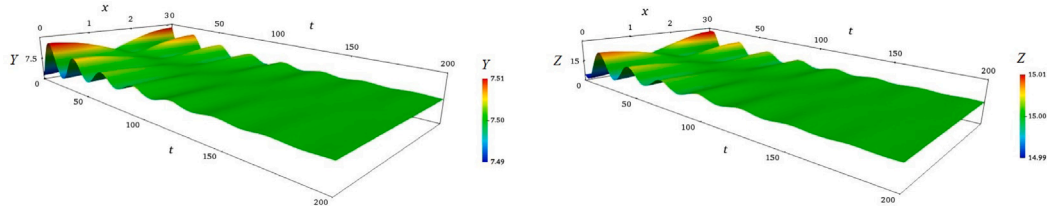

Fig. 13. Spatio-temporal graph of density of prey (left), spatio-temporal graph of density of predator (right). Here, diffusion coefficients are $d_1 = 0.01$ and $d_2 = 0.005$. The initial conditions are $Y(x,0) = 7.5 - 0.01\cos(x)$, $Z(x,0) = 15 - 0.01\cos(x)$. The delay values are $\tau_2 = 2$ and $\tau_1 = 1.5 \in [0, 2.6815)$. Simulations illustrate the asymptotic stability of the equilibrium point for $\tau_2 < \tau_{2_0} = 3.9557$ when $\tau_1 = 1.5$.

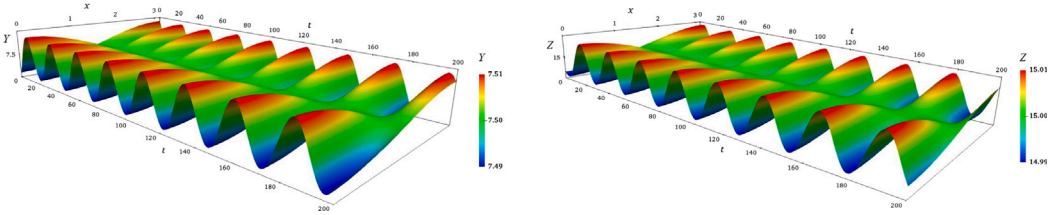

Fig. 14. Spatio-temporal graph of density of prey (left), spatio-temporal graph of density of predator (right). Here, diffusion coefficients are $d_1 = 0.01$ and $d_2 = 0.005$. The initial conditions are $Y(x,0) = 7.5 - 0.01\cos(x)$, $Z(x,0) = 15 - 0.01\cos(x)$. The delay values are $\tau_2 = 3.9560$ and $\tau_1 = 1.5 \in [0, 2.6815)$. From these simulations one can observe that as τ_2 passes through the critical value $\tau_2 \approx 3.9557$ a Hopf bifurcation arises at the equilibrium point $P^\star = (7.5, 15)$ when $\tau_1 = 1.5$.

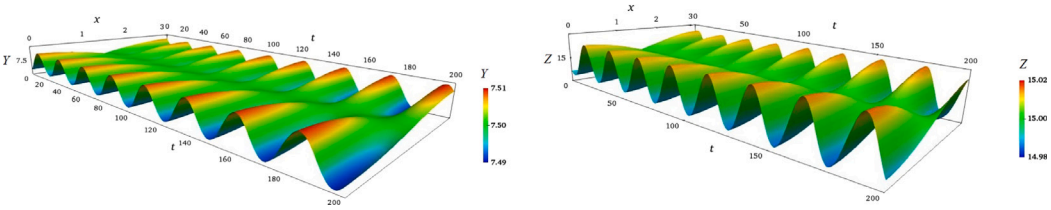

Fig. 15. Spatio-temporal graph of density of prey (left), spatio-temporal graph of density of predator (right). Here, diffusion coefficients are $d_1 = 0.01$ and $d_2 = 0.005$. The initial conditions are $Y(x,0) = 7.5 - 0.01\cos(x)$, $Z(x,0) = 15 - 0.01\cos(x)$. The delay values are $\tau_2 = 4.05$ and $\tau_1 = 1.5 \in [0, 2.6815)$. Simulations demonstrate the nonlinear instability of the equilibrium point for $\tau_2 < \tau_{2_0} = 3.9557$ when $\tau_1 = 1.5$.

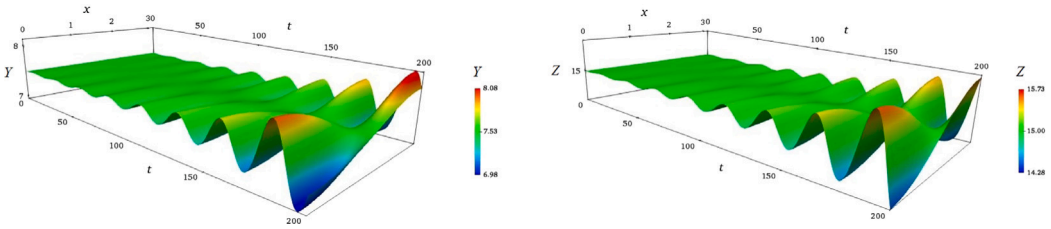

Fig. 16. Spatio-temporal graph of density of prey (left), spatio-temporal graph of density of predator (right). Here, diffusion coefficients are $d_1 = 0.01$ and $d_2 = 0.005$. The initial conditions are $Y(x,0) = 7.5 - 0.01\cos(x)$, $Z(x,0) = 15 - 0.01\cos(x)$. The delay values are $\tau_2 = 5.36$ and $\tau_1 = 1.5 \in [0, 2.6815)$. Simulations demonstrate the instability of the equilibrium point for $\tau_2 > \tau_{2_0} = 3.9557$ when $\tau_1 = 1.5$.

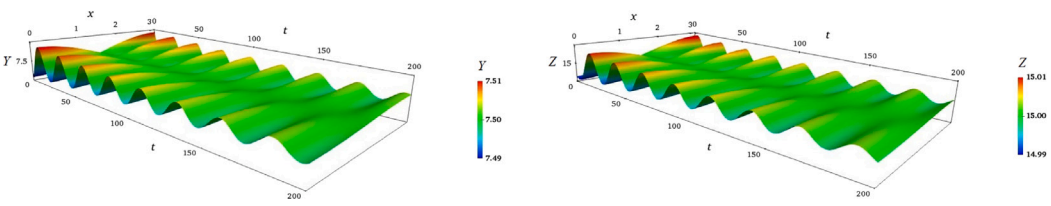

Fig. 17. Spatio-temporal graph of density of prey (left), spatio-temporal graph of density of predator (right). Here, diffusion coefficients are $d_1 = 0.01$ and $d_2 = 0.01$. The initial conditions are $Y(x,0) = 7.5 - 0.01\cos(x)$, $Z(x,0) = 15 - 0.01\cos(x)$. The delay values are $\tau_2 = 3.7$ and $\tau_1 = 1.5 \in [0, 2.8097)$. Simulations illustrate the asymptotic stability of the equilibrium point for $\tau_2 < \tau_{2_0} = 4.1562$ when $\tau_1 = 1.5$.

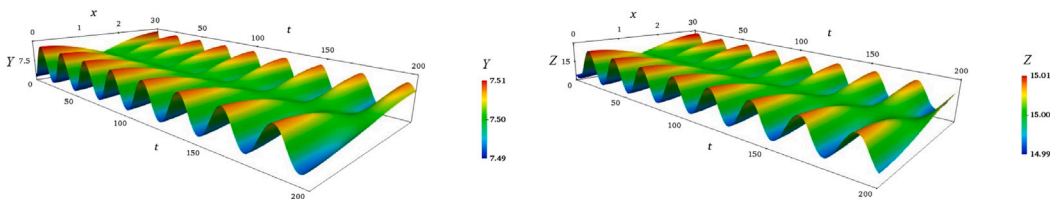

Fig. 18. Spatio-temporal graph of density of prey (left), spatio-temporal graph of density of predator (right). Here, diffusion coefficients are $d_1 = 0.01$ and $d_2 = 0.01$. The initial conditions are $Y(x,0) = 7.5 - 0.01\cos(x)$, $Z(x,0) = 15 - 0.01\cos(x)$. The delay values are $\tau_2 = 4.05$ and $\tau_1 = 1.5 \in [0, 2.8097)$. Simulations illustrate the nonlinearly asymptotic stability of the equilibrium point for $\tau_2 < \tau_{2_0} = 4.1562$ when $\tau_1 = 1.5$.

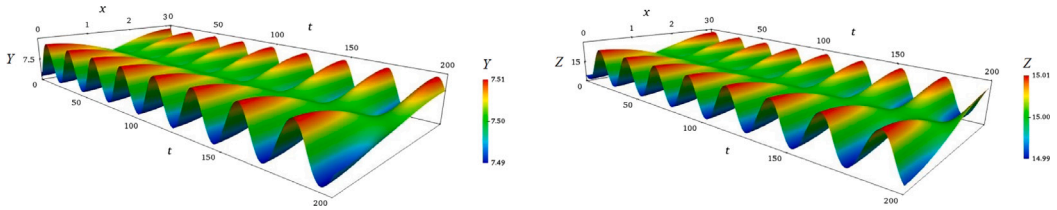

Fig. 19. Spatio-temporal graph of density of prey (left), spatio-temporal graph of density of predator (right). Here, diffusion coefficients are $d_1 = 0.01$ and $d_2 = 0.01$. The initial conditions are $Y(x,0) = 7.5 - 0.01\cos(x)$, $Z(x,0) = 15 - 0.01\cos(x)$. The delay values are $\tau_2 = 4.1560$ and $\tau_1 = 1.5 \in [0, 2.8097)$. From these simulations one can observe that as τ_2 passes through the critical value $\tau_2 \approx 4.1562$ a Hopf bifurcation arises at the equilibrium point $P^\star = (7.5, 15)$ when $\tau_1 = 1.5$.

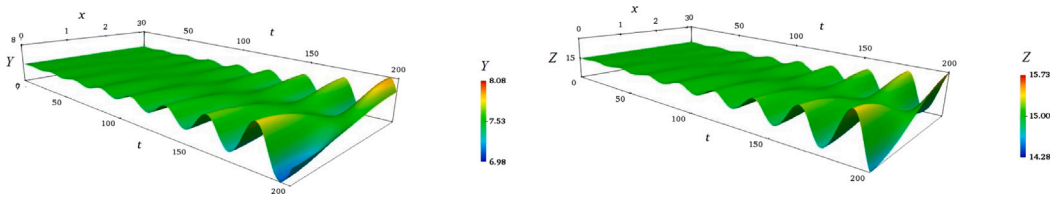

Fig. 20. Spatio-temporal graph of density of prey (left), spatio-temporal graph of density of predator (right). Here, diffusion coefficients are $d_1 = 0.01$ and $d_2 = 0.01$. The initial conditions are $Y(x,0) = 7.5 - 0.01\cos(x)$, $Z(x,0) = 15 - 0.01\cos(x)$. The delay values are $\tau_2 = 5.5$ and $\tau_1 = 1.5 \in [0, 2.8097)$. Simulations demonstrate the instability of the equilibrium point for $\tau_2 > \tau_{2_0} = 4.1562$ when $\tau_1 = 1.5$.

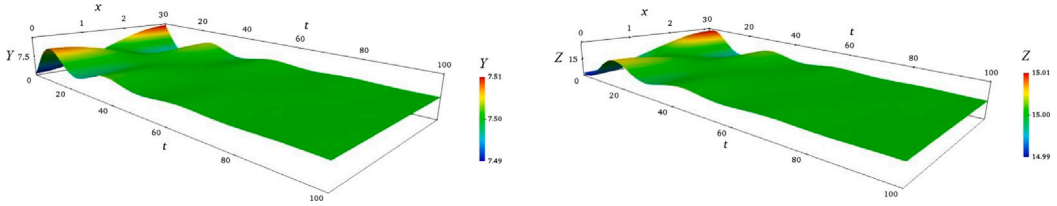

Fig. 21. Spatio-temporal graph of density of prey (left), spatio-temporal graph of density of predator (right). Here, diffusion coefficients are $d_1 = 0.01$ and $d_2 = 0.05$. The initial conditions are $Y(x,0) = 7.5 - 0.01\cos(x)$, $Z(x,0) = 15 - 0.01\cos(x)$. The delay values are $\tau_2 = 2$ and $\tau_1 = 1.5 \in [0, 3.8908)$. Simulations illustrate the asymptotic stability of the equilibrium point for $\tau_2 < \tau_{2_0} = 5.6476$ when $\tau_1 = 1.5$.

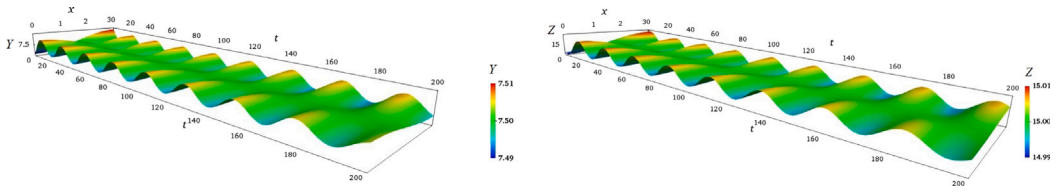

Fig. 22. Spatio-temporal graph of density of prey (left), spatio-temporal graph of density of predator (right). Here, diffusion coefficients are $d_1 = 0.01$ and $d_2 = 0.05$. The initial conditions are $Y(x,0) = 7.5 - 0.01\cos(x)$, $Z(x,0) = 15 - 0.01\cos(x)$. The delay values are $\tau_2 = 5.5$ and $\tau_1 = 1.5 \in [0, 3.8908)$. Simulations illustrate the nonlinearly asymptotic stability of the equilibrium point for $\tau_2 < \tau_{2_0} = 5.6476$ when $\tau_1 = 1.5$.

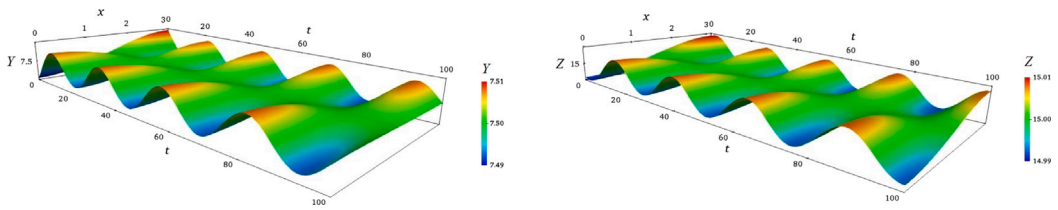

Fig. 23. Spatio-temporal graph of density of prey (left), spatio-temporal graph of density of predator (right). Here, diffusion coefficients are $d_1 = 0.01$ and $d_2 = 0.05$. The initial conditions are $Y(x,0) = 7.5 - 0.01\cos(x)$, $Z(x,0) = 15 - 0.01\cos(x)$. The delay values are $\tau_2 = 5.6476$ and $\tau_1 = 1.5 \in [0, 3.8908)$. From these simulations one can observe that as τ_2 passes through the critical value $\tau_2 = 5.6476$ a Hopf bifurcation arises at the equilibrium point $P^\star = (7.5, 15)$ when $\tau_1 = 1.5$.

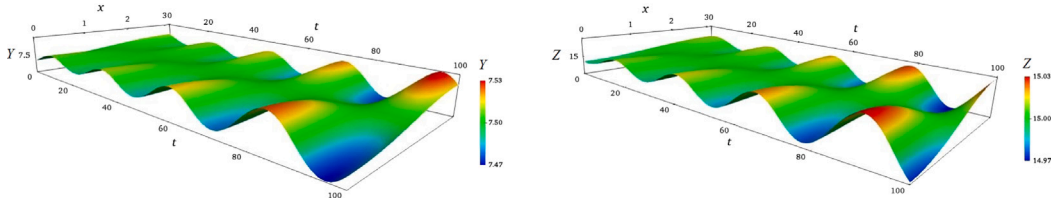

Fig. 24. Spatio-temporal graph of density of prey (left), spatio-temporal graph of density of predator (right). Here, diffusion coefficients are $d_1 = 0.01$ and $d_2 = 0.05$. The initial conditions are $Y(x,0) = 7.5 - 0.01\cos(x)$, $Z(x,0) = 15 - 0.01\cos(x)$. The delay values are $\tau_2 = 7$ and $\tau_1 = 1.5 \in [0, 3.8908)$. Simulations demonstrate the instability of the equilibrium point for $\tau_2 > \tau_{2_0} = 5.6476$ when $\tau_1 = 1.5$.

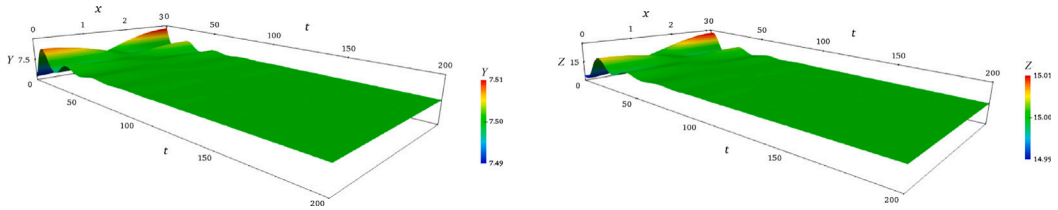

Fig. 25. Spatio-temporal graph of density of prey (left), spatio-temporal graph of density of predator (right). Here, diffusion coefficients are $d_1 = 0.01$ and $d_2 = 0.005$. The initial conditions are $Y(x,0) = 7.5 - 0.01\cos(x)$, $Z(x,0) = 15 - 0.01\cos(x)$. The delay values are $\tau_2 = 2$ and $\tau_1 = 0.5 \in [0, 2.6815)$. Simulations illustrate the asymptotic stability of the equilibrium point for $\tau_2 < \tau_{2_0} = 5.4642$ when $\tau_1 = 0.5$.

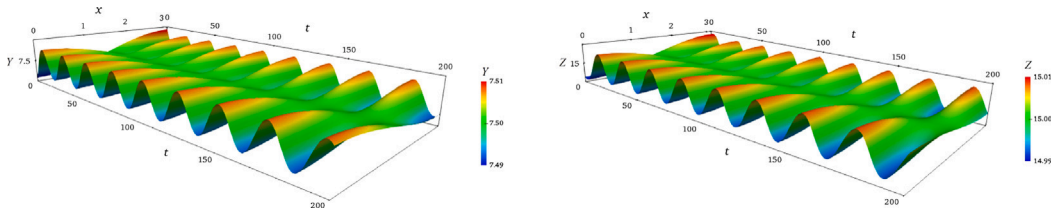

Fig. 26. Spatio-temporal graph of density of prey (left), spatio-temporal graph of density of predator (right),. Here, diffusion coefficients are $d_1 = 0.01$ and $d_2 = 0.005$. The initial conditions are $Y(x,0) = 7.5 - 0.01\cos(x)$, $Z(x,0) = 15 - 0.01\cos(x)$. The delay values are $\tau_2 = 5.4642$ and $\tau_1 = 0.5 \in [0, 2.6815)$. From these simulations one can observe that as τ_2 passes through the critical value $\tau_2 = 5.4642$ a Hopf bifurcation arises at the equilibrium point $P^\star = (7.5, 15)$ when $\tau_1 = 0.5$.

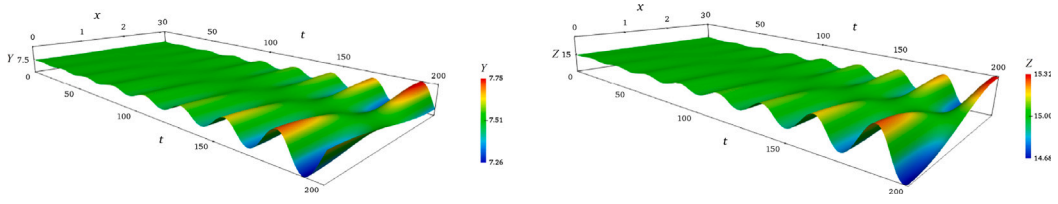

Fig. 27. Spatio-temporal graph of density of prey (left), spatio-temporal graph of density of predator (right). Here, diffusion coefficients are $d_1 = 0.01$ and $d_2 = 0.005$. The initial conditions are $Y(x,0) = 7.5 - 0.01\cos(x)$, $Z(x,0) = 15 - 0.01\cos(x)$. The delay values are $\tau_2 = 7$ and $\tau_1 = 0.5 \in [0, 2.6815)$. Simulations demonstrate the instability of the equilibrium point for $\tau_2 > \tau_{2_0} = 5.4642$ when $\tau_1 = 0.5$.

that the dynamic can repeat itself. And this repetition, which means continuing to live together, occurs over a shorter period.

In order to investigate the effect of the time required for the prey species to reach maturity (τ_1) on the population dynamics represented by the system (4.2), the diffusion coefficient values are fixed as $d_1 = 0.01$ and $d_2 = 0.005$ (as in case **(C4)**). If we increase the value of τ_1 when $d_1 = 0.01$ and $d_2 = 0.005$, the following changes in the dynamics of the system (4.2) are observed: (i) the equilibrium point remains stable for a more shorter period according to the predator's ability to hunt (τ_2), (ii) periodic solutions occur at an earlier time (τ_2) required for the predator to be capable of hunting, and (iii) the period of the periodic solutions increases. These ecologically means that, if

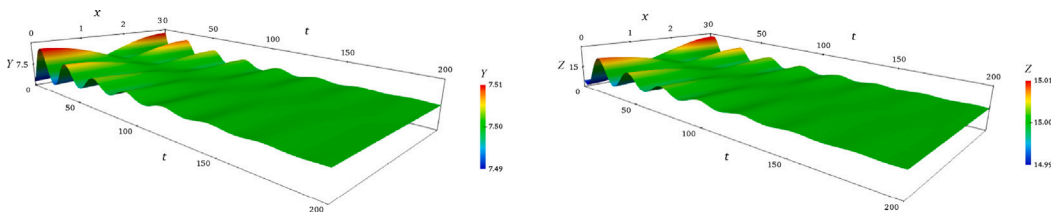

Fig. 28. Spatio-temporal graph of density of prey (left), spatio-temporal graph of density of predator (right). Here, diffusion coefficients are $d_1 = 0.01$ and $d_2 = 0.005$. The initial conditions are $Y(x,0) = 7.5 - 0.01\cos(x)$, $Z(x,0) = 15 - 0.01\cos(x)$. The delay values are $\tau_2 = 2$ and $\tau_1 = 1.5 \in [0, 2.6815)$. Simulations illustrate the asymptotic stability of the equilibrium point for $\tau_2 < \tau_{2_0} = 3.9557$ when $\tau_1 = 1.5$.

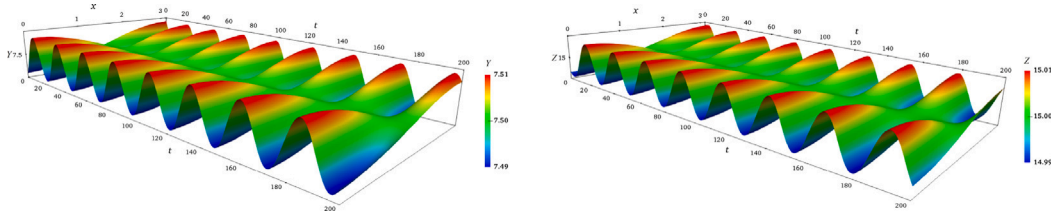

Fig. 29. Spatio-temporal graph of density of prey (left), spatio-temporal graph of density of predator (right). Here, diffusion coefficients are $d_1 = 0.01$ and $d_2 = 0.005$. The initial conditions are $Y(x,0) = 7.5 - 0.01\cos(x)$, $Z(x,0) = 15 - 0.01\cos(x)$. The delay values are $\tau_2 = 3.956$ and $\tau_1 = 1.5 \in [0, 2.6815)$. From these simulations one can observe that as τ_2 passes through the critical value $\tau_2 \approx 3.9557$ a Hopf bifurcation arises at the equilibrium point $P^\star = (7.5, 15)$ when $\tau_1 = 1.5$.

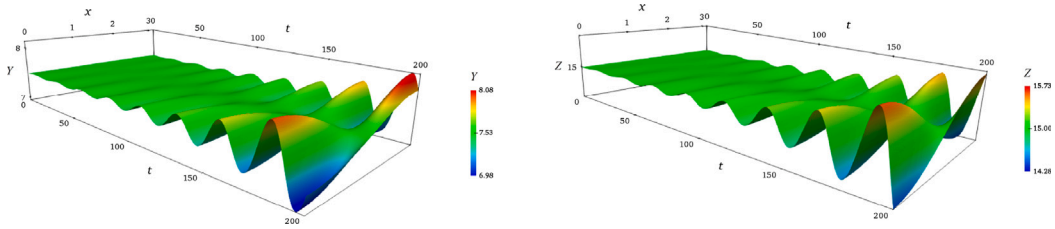

Fig. 30. Spatio-temporal graph of density of prey (left), spatio-temporal graph of density of predator (right). Here, diffusion coefficients are $d_1 = 0.01$ and $d_2 = 0.005$. The initial conditions are $Y(x,0) = 7.5 - 0.01\cos(x)$, $Z(x,0) = 15 - 0.01\cos(x)$. The delay values are $\tau_2 = 5.36$ and $\tau_1 = 1.5 \in [0, 2.6815)$. Simulations demonstrate the instability of the equilibrium point for $\tau_2 > \tau_{2_0} = 3.9557$ when $\tau_1 = 1.5$.

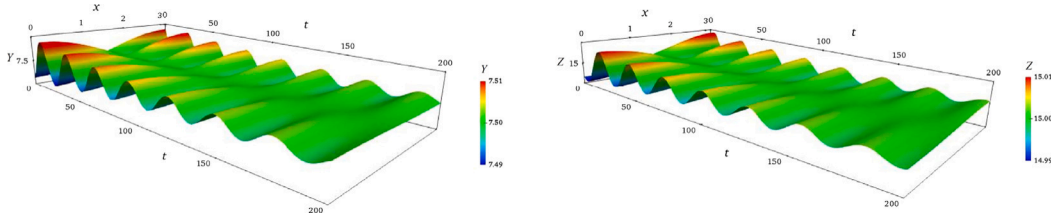

Fig. 31. Spatio-temporal graph of density of prey (left), spatio-temporal graph of density of predator (right). Here, diffusion coefficients are $d_1 = 0.01$ and $d_2 = 0.005$. The initial conditions are $Y(x,0) = 7.5 - 0.01\cos(x)$, $Z(x,0) = 15 - 0.01\cos(x)$. The delay values are $\tau_2 = 2$ and $\tau_1 = 2 \in [0, 2.6815)$. Simulations illustrate the asymptotic stability of the equilibrium point for $\tau_2 < \tau_{2_0} = 3.0709$ when $\tau_1 = 2$.

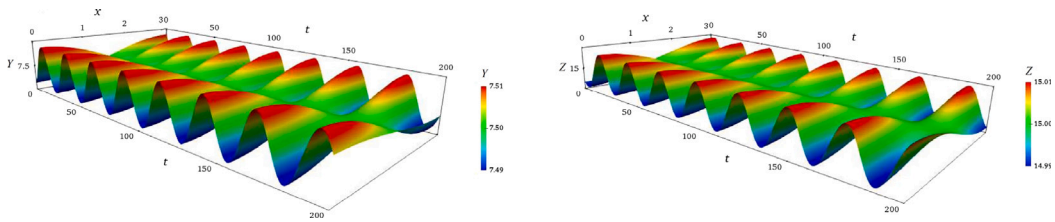

Fig. 32. Spatio-temporal graph of density of prey (left), spatio-temporal graph of density of predator (right). Here, diffusion coefficients are $d_1 = 0.01$ and $d_2 = 0.005$. The initial conditions are $Y(x,0) = 7.5 - 0.01\cos(x)$, $Z(x,0) = 15 - 0.01\cos(x)$. The delay values are $\tau_2 = 3.071$ and $\tau_1 = 2 \in [0, 2.6815)$. From these simulations one can observe that as τ_2 passes through the critical value $\tau_2 \approx 3.0709$ a Hopf bifurcation arises at the equilibrium point $P^\star = (7.5, 15)$ when $\tau_1 = 2$.

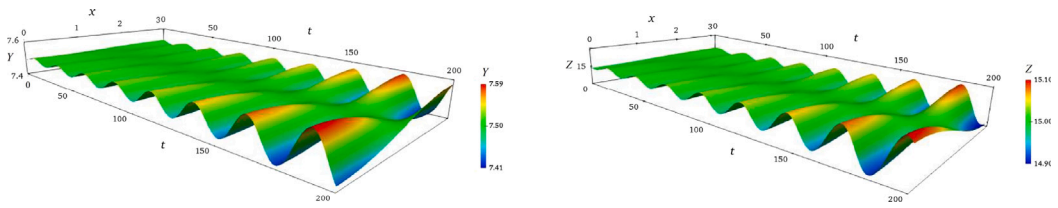

Fig. 33. Spatio-temporal graph of density of prey (left), spatio-temporal graph of density of predator (right). Here, diffusion coefficients are $d_1 = 0.01$ and $d_2 = 0.005$. The initial conditions are $Y(x,0) = 7.5 - 0.01\cos(x)$, $Z(x,0) = 15 - 0.01\cos(x)$. The delay values are $\tau_2 = 3.95$ and $\tau_1 = 2 \in [0, 2.6815)$. Simulations demonstrate the instability of the equilibrium point for $\tau_2 > \tau_{2_0} = 3.0709$ when $\tau_1 = 2$.

the prey and predator species move randomly with a constant diffusion coefficients $d_1 = 0.01$ and $d_1 = 0.005$, respectively, when the prey needs longer time to mature, the predator needs to gain the ability to hunt earlier so that the dynamic can repeat itself. And this repetition, which means living together, occurs over a more extended period.

CRediT authorship contribution statement

Ş. Bilazeroğlu: Conceptualization, Methodology, Software, Writing – original draft, Writing – review & editing, Investigation. **S. Göktepe:** Software, Writing – review & editing. **H. Merdan:** Conceptualization, Methodology, Software, Writing – review & editing, Supervision, Investigation.

Declaration of competing interest

We wish to confirm that there are no known conflicts of interest associated with this publication and there has been no significant financial support for this work that could have influenced its outcome.

Data availability

No data was used for the research described in the article.

References

[1] Akçakaya H, Arditi R, Ginzburg L. Ratio-dependent predation: an abstraction that works. Ecology 1995;76(3):995–1004.

[2] Abrams P, Ginzburg L. The nature of predation: prey dependent, ratio-dependent or neither? Trends Ecol Evol 2000;15(8):337–41.

[3] Bandyopadhyay M, Chattopadhyay J. Ratio-dependent predator-prey model: effect of environmental fluctuation and stability. Nonlinearity 2005;18(2):913. http://dx.doi.org/10.1088/0951-7715/18/2/022.

[4] Akçakaya H. Population cycles of mammals: evidence for a ratio-dependent predation hypothesis. Ecol Monograph 1992;62:119–42.

[5] Anisiu M. Lotka, Volterra and their model. Didact Math 2014;32:9–17.

[6] Lotka A. Analytical note on certain rhythmic relations in organic systems. Proc Natl Acad Sci 1920;6:410–5.

[7] Volterra V. Fluctuations in the abundance of a species considered mathematically. Nature 1926;118:558–60.

[8] Holling C. Some characteristics of simple types of predation and parasitism. Can Entomol 1959;91(7):385–98.

[9] Rosenzweig M, MacArthur R. Graphical representation and stability conditions of predator-prey interactions. Am Nat 1963;97:217–23.

[10] Hassell M, Varley G. New inductive population model for insect parasites and its bearing on biological control. Nature 1969;223:1133–7.

[11] DeAngelis D, Goldstein R, O'Neill R. A model for tropic interaction. Ecology 1975;56(4):881–92.

[12] Getz W. Population dynamics: a per capita resource approach. J Theoret Biol 1984;108(4):623–43.

[13] Arditi R, Ginzburg L. Coupling in predator prey dynamics: ratio-dependence. J Theoret Biol 1989;139:311–26.

[14] Leslie P. Some further notes on the use of matrices in population mathematics. Biometrika 1948;35:213–45.

[15] Gause G. The struggle for existence. Baltimore: Williams and Wilkins; 1934.

[16] Zhou S, Liu Y, Wang G. The stability of predator-prey systems subject to the Allee effects. Theor Popul Biol 2005;67:23–31.

[17] Çelik C. The stability and hopf bifurcation for a predator-prey system with time delay. Chaos Solitons Fractals 2008;37:87–99. http://dx.doi.org/10.1016/j.chaos.2007.10.045.

[18] Çelik C. Hopf bifurcation of a ratio-dependent predator-prey system with time delay. Chaos Solitons Fractals 2009;42:1474–84. http://dx.doi.org/10.1016/j.chaos.2009.03.071.

[19] Karaoğlu E, Merdan H. Hopf bifurcations of a ratio-dependent predator–prey model involving two discrete maturation time delays. Chaos Solitons Fractals 2014;68:159–68.

[20] Karaoğlu E, Merdan H. Hopf bifurcation analysis for a ratio-dependent predator-prey system involving two delays. ANZIAM J 2014;55:214–31.

[21] Hassard B, Kazarinoff N, Wan Y. Theory and application of Hopf bifurcation. Cambridge: Cambridge Univ. Press; 1981.

[22] Malchow H, Petrovskii S, Venturino E. Spatiotemporal patterns in ecology and epidemiology: Theory, models, and simulation. Chapman and Hall/CRC; 2007.

[23] Root R, Kareiva P. The search for resources by cabbage butterflies (pieris rapae): Ecological consequences and adaptive significance of Markovian movements in a patchy environment. Ecology 1984;65(1):147–65.

[24] Brockmann D, Hufnagel L, Geisel T. The scaling laws of human travel. Nature 2006;462–5.

[25] Allen L. An introduction to mathematical biology. New Jersey: Upper Saddle River, Pearson-Prentice Hall; 2007.

[26] Wang F, Yang R. Spatial pattern formation driven by the cross-diffusion in a predator–prey model with holling type functional response. Chaos Solitons Fractals 2023;174:113890. http://dx.doi.org/10.1016/j.chaos.2023.113890.

[27] Yang R, Nie C, Jin D. Spatiotemporal dynamics induced by nonlocal competition in a diffusive predator-prey system with habitat complexity. Nonlinear Dyn 2002;110:879–900. http://dx.doi.org/10.1007/s11071-022-07625-x.

[28] Yang R, Wang F, Jin D. Spatially inhomogeneous bifurcating periodic solutions induced by nonlocal competition in a predator–prey system with additional food. Math Methods Appl Sci 2022;45(16):9967–78. http://dx.doi.org/10.1002/mma.8349.

[29] Hu G, Li W. Hopf bifurcation analysis for a delayed predator–prey system with diffusion effects. Nonlinear Anal RWA 2010;11(2):819–26.

[30] Bilazeroğlu S, Merdan H. Hopf bifurcations in a class of reaction-diffusion equations including two discrete time delays: An algorithm for determining hopf bifurcation, and its applications. Chaos Solitons Fractals 2021;142:110391. http://dx.doi.org/10.1016/j.chaos.2020.110391.

[31] Kayan S, Merdan H. An algorithm for hopf bifurcation analysis of a delayed reaction-diffusion model. Nonlinear Dyn 2017;89:345–66. http://dx.doi.org/10.1007/s11071-017-3458-5.

[32] Taylor RL. FEAP - Finite element analysis program. Berkeley: University of California; 2014, URL http://www.ce.berkeley/feap.